Original Article

The Possible Protective Effect of Vorinostat Versus Metformin on a Rat Model of New-Onset Post Transplantation Diabetes: Histological, Immunohistochemical, and Biochemical Study

Heba Fikry[1], Lobna A. Saleh[2], Hadwa Ali Abd Alkhalek[1] and Doaa R. Sadek[1]

[1]Department of Histology and Cell Biology, [2]Department of Clinical Pharmacology. Faculty of Medicine, Ain Shams University, Cairo, Egypt

ABSTRACT

Background: One of the most popular immunosuppressants used for organ transplants is tacrolimus. New-onset diabetes after transplantation (NODAT) occurs when patient develops diabetes mellitus (DM) following a solid organ transplant. The impact of metformin on newly-onset diabetes following transplantation due to immunosuppressant treatment is not well understood, even though it is a first-line medicine for type 2 DM.

Aim: To demonstrate the possible protective effects of vorinostat versus metformin against diabetic nephropathy in the tacrolimus-induced NODAT rat model.

Materials and Methods: Forty-two adult male rats were randomly divided into six groups: negative control, vorinostat, metformin, NODAT rat model (induced by tacrolimus), NODAT + vorinostat, and NODAT + metformin. High dose of tacrolimus was given by subcutaneous injection for four weeks to develop NODAT. Vorinostat and metformin were concomitantly given with tacrolimus to rats of group 5 and 6 for 4 weeks. At the end of the experiment after 4weeks, blood samples were collected to measure kidney function. kidneys were subjected to histological, immunohistochemical, histomorphometric examination as well as measuring of oxidative stress markers.

Results: in NODAT group, there was a discernible increase in the weight of the kidneys, which was successfully halted with administration of vorinostat. H&E, Masson trichrome, PAS, and Gordon & Sweets' silver impregnation staining revealed statistically significant kidney injuries. Rats given tacrolimus as the only treatment had significantly higher levels of caspase-3 reaction in their proximal tubular cells. It was significantly reduced in rats treated with vorinostat as compared to the metformin-treated rats. The most important finding of this study was that vorinostat and metformin treatment caused different glucose-lowering effects. Metformin improved this condition, but not to the degree seen in vorinostat.

Conclusion: Vorinostat was more effective than metformin in protecting rat kidneys against tacrolimus-induced NODAT rat model. Vorinostat controlled diabetic kidney damage by increasing antioxidant capacity, decreasing oxidative damage, and decreasing apoptosis. Therefore, Vorinostat showed a double-edged sword: it prevented kidney damage and improved biochemical outcomes.

Key Words: Caspase-3, histological, kidney, metformin, MDA, NODAT, rat, vorinostat.

Received: 22 April 2025, **Accepted:** 26 May 2025.

Corresponding Author: Doaa R. Sadek, Department of Histology and Cell Biology, Faculty of Medicine, Ain Shams University, Cairo, Egypt., **Tel.:** +201002609026, **E-mail**: d.sadek@med.asu.edu.eg

ISSN: 2735-3540, Vol. 76, No. 3, Sep. 2025.

INTRODUCTION

Donation recipients are at increased risk for developing New-onset diabetes after transplantation (NODAT), a devastating metabolic complication that shortens both the patient's and the donor's life expectancy after a solid organ donation[1,2]. The prevalence of NODAT may range from 2 to 53% of the population. Many negative consequences, including increased infection rates, early graft loss, decreased patient survival, and an increased risk of death and cardiovascular events, are associated with patients developing NODAT[1,3]. It has been observed that NODAT occurs in a range of organ transplant recipients, including kidneys (4-5%), livers (2.5-25%), hearts (4-40%), and lungs (30-35%)[4].

One class of immunomodulatory drugs used to treat autoimmune diseases, glomerulonephritis, and post-transplant complications are calcineurin inhibitors (CNIs), which include tacrolimus and cyclosporine. Up until now, the majority of CNIs have concentrated on people who have recently received a transplant[5]. One of the most widely used immunosuppressants for preventing immune rejection

DOI: 10.21608/ASMJ.2025.377846.1440

following organ donation is tacrolimus, an essential CNI[6]. Several metabolic issues, such as dyslipidemia and post-transplantation diabetic mellitus (PTDM), are linked to its clinically advised dosage[7]. In addition to increasing the likelihood of cardiovascular disease and serious diabetes-related problems, these issues are known to lower organ transplant recipients' quality of life and cause graft malfunction [8]. According to most of the relevant research, the high mean tacrolimus concentration is related to an increased risk of PTDM, Tacrolimus has a higher chance of generating PTDM than cyclosporine [9].

The kidney, the second most important organ in systemic glucose metabolism after the liver, regulates glucose reabsorption and gluconeogenesis [10]. The kidney is responsible for 40% of glucose absorption when fasting, suggesting that renal damage or aberrant gene expression plays a significant role in the development of diabetes mellitus and PTDM, as gluconeogenesis exclusively occurs in the liver and kidney [11]. Evidence from animal studies suggests that tacrolimus post-transplantation may cause PTDM-related complications such as progressive renal failure characterized by striped interstitial fibrosis, tubular atrophy, inflammatory cell infiltration, and hyalinosis of the afferent arterioles [12].

Those without a transplant currently have metformin, an oral biguanide, as their first line of treatment against type 2 diabetes mellitus (T2DM) [13]. Its antidiabetic effect is achieved through many pathways [14]. The usage of metformin following solid organ transplantation is gaining more and more attention [15]. Several organs, including the kidneys, have been found to be protected from fibrosis by metformin [16,17]. However, patients with chronic kidney illness choose to avoid it because of worries about lactic acidosis and medication accumulation. Metformin-associated lactic acidosis is very uncommon but has a fatality rate of more than 50% because to its renal excretion. Metformin-associated lactic acidosis is substantially more likely to occur in patients with renal impairment [18,19]. Metformin is contraindicated in patients with diabetic ketoacidosis or diabetic precoma, renal dysfunction, and acute conditions which have the potential for altering renal function such as: dehydration, severe infection, and shock[20].

Researchers have been looking at therapeutic repurposing prospects, such as studying drugs in the histone deacetylase inhibitor (HDACi) class, as a potential treatment [21]. Vorinostat is an HDACi, that was approved by the FDA in 2006 to treat persistent and relapsed cutaneous T-cell lymphoma [22]. However, its anti-inflammatory effects have been appreciated. Indeed, it has been defined as one of the broad-spectrum of HDACi with anti-inflammatory and antioxidant characteristics [23]. In addition, studies conducted on animal models of Type 1 DM have shown that vorinostat has an anti-diabetic impact [24,25]. As a result of its many positive characteristics, Vorinostat is a promising therapeutic option for the treatment of NODAT in kidney transplant recipients.

Therefore, the current study aimed to administering a daily high dose of tacrolimus (an immunosuppressant medication used following organ transplantation) to male Wistar albino rats for four weeks to develop NODAT, then demonstrate the possible protective effects of vorinostat in contrast to metformin against tacrolimus-induced NODAT rat model.

MATERIALS & METHODS

Drugs

Tacrolimus (Prograf®, 1 mg, Astellas Pharma US, Inc. Northbrook, IL 60062) (details of the drug) was purchased from local pharmacy, Cairo, Egypt. Tacrolimus powder was dissolved in a mixture of 100% ethanol (8% of total volume), olive oil (2% of total volume), and sterile saline for injections until the final concentration reached 1.5 mg/ml [26]. ***Hwang et al.*** [27] found that blood glucose levels increased dose-dependently by intraperitoneal glucose tolerance testing (IPGTT), so we decided to use 1.5 mg/kg of tacrolimus in this investigation.

Vorinostat powder (cat. 149647-78-9) was purchased from Sigma-Aldrich (St. Louis, MO, USA). The purity of the drug was 99.6%. Vorinostat dose (50 mg/kg) was chosen based on previous reports by ***Advani et al.*** [28] and ***Gilbert et al.*** [29]. As part of the safety pharmacology studies, which included cardiovascular, respiratory, and functional observational battery studies, oral dosage formulations of vorinostat were produced as suspensions in a vehicle of 0.5 ml of 0.5% Dimethyl sulfoxide (DMSO) and administered to each rat at a volume of 5 mL/kg daily by gastric gavage using intragastric tube. The formulations were made every day and kept constantly mixed while they were being used[30].

Metformin powder (Metformin hydrochloride, CAS No.: 1115-70-4) was purchased from Sigma-Aldrich, St. Louis, MO, USA. A previous research has shown that metformin doses of 100 and 200 mg/kg are beneficial in glucose management, thus that is 200 mg/kg the amount that was chosen [31]. Clinical indications of toxicity can be observed when metformin dosages are 600 mg/kg/day or higher [32]. Metformin hydrochloride, 200 mg, was dissolved in 4 ml of distilled water and given to the adult rat. For four weeks, one dose of either distilled water alone (control) or rats were given 200 mg/kg of metformin diluted in distilled water (metformin control group and metformin treated group) through intragastric once a day. Metformin toxicity was not an issue with the dosages utilized in this study, suggesting that they are appropriate for blood glucose control. Daily therapeutic doses for humans varied between 500 and 2550 mg [33].

Animals

In our study, forty-two adult male Wistar albino rats (5-7 months) with an average body weight ranging from (200–250 g) were used. They were from the breading animal house, Faculty of Medicine, Ain Shams University.

ETHICAL CONSIDERATION

The research ethics committee at the Faculty of Medicine, Ain Shams University approved the experimental protocol. The approval number was (FMASU- R224/2022). The animals were given free access to tap water and a low-salt diet (0.05% sodium) to avoid another risk factor (hypertension) at a standard temperature with regular dark and light cycles while being housed.

Study Design

After acclimating to the lab setting for a week, thirty-six rats were allocated randomly to one of six groups. With six rats in each group, except for group 1 which included ten rats.

Group 1 (G1): was divided into two equal subgroups. G1a negative control: which had no intervention. G1b Positive control: rats were given daily subcutaneous injection of 1ml (10% ethanol and 90% olive oil solution). Rats were concomitantly given 1 ml DMSO by oral gavage using gastric tube daily for 4 weeks.

Group 2 (G2, vorinostat control): Rats received vorinostat (50 mg/kg) once daily by oral gavage of for 4 weeks according to ***Advani et al.*** [28] and ***Gilbert et al.***[29].

Group 3 (G3, metformin control): For four weeks, rats were given 200 mg/kg of metformin diluted in distilled water through intragastric tube once a day [31].

Group 4 NODAT model (G4, NODAT model group): Rats received daily subcutaneous injection of tacrolimus (1.5 mg/kg) for 4 weeks [34].

Group 5 (G5, NODAT model + Vorinostat group): Rats were treated with tacrolimus as in group 4. Rats were treated with vorinostat as in group 2 for 4 weeks.

Group 6 (G6, NODAT model + Metformin group): Rats were given tacrolimus as in group 4 and concomitantly given metformin as in group 3 for 4 weeks.

At the end of the experiment (4weeks), the animals were euthanized, and blood and kidney samples were obtained. Animals were sedated with a mixture of ketamine (75 mg/kg) and xylazine (5 mg/kg) administered via intraperitoneal (i.p.) injection. A midline upper abdominal incision was performed, and the kidney was dissected. Kidney weights were measured, and the relative kidney/body weight ratio was calculated [35]. Blood was collected from retroorbital vein. A midline upper abdominal incision was performed, and the kidney was dissected. Kidney weights were measured, and the relative kidney/body weight ratio was calculated [36]. The right kidneys were used for histological studies and the left kidneys were used for tissue homogenate for biochemical studies.

Body Weight Changes

The body weight of each rat in all groups was measured and recorded at the beginning (day 0) and after four weeks (at the end of the experiment) for each rat in the corresponding group.

Assessment of developing diabetes parameters in the NODAT rat model.

1. **Measurement of fasting blood glucose (FBG) level.**

A sterile needle was used to draw blood from the tail vein, and a one-touch ultra-glucometer (Boehringer-Mannheim, Germany) was used to assess glucose levels after 8-hours fast on day 0 and week 4.

2. **The intraperitoneal Glucose tolerance test (IPGTT)**

Following the protocols laid out by ***Le et al.*** [37] and ***Mooli et al.*** [38], we administered an intraperitoneal glucose tolerance test (IPGTT) to rats at week 4. In the IPGTT, rats were given a 8-hour fast before having their blood glucose levels checked with a glucometer. Then, at 0,15, 30-, 60-, and 120-minutes following injection, they were given 20% glucose intraperitoneally (2 g/kg body weight), and their blood glucose levels were monitored via the lateral tail vein.

Biochemical analysis

1. **Blood samples:**

At the end of the experiment, blood samples were taken under ether light anaesthesia in non-heparinized tubes from the retro-orbital veins of each rat in all groups. Centrifuging serum at 4000 g for 20 minutes and storing it at 20°C was the method used to separate the serum. The levels of blood plasma insulin (with the rat/mouse insulin ELISA, Catalog number: 635151, purchased from Sigma, St. Louis, MO, USA), urea, and serum creatinine (Catalog number: EIABUN colorimetric kits purchased from Bio-diagnostic Co., Giza, Egypt) were measured following the manufacturer's information.

2. **Tissue homogenate samples:**

The left kidney of each animal was subsequently homogenized in ice-cold 0.15 M KCl using a sonicator

homogenizer to create a 10% homogenate, which was then centrifuged and utilized to estimate the levels of oxidative stress marker and total antioxidant capacity (TAC) in renal tissue homogenate. Colorimetric measurements of Malondialdehyde (MDA) (a marker of lipid peroxidation), and Total antioxidant capacity (TAC) using a readily available kit, (Biodiagnostic, Cairo, Egypt) were made in kidney homogenate. The values in each group were determined in the centrifuged homogenates supernatant. All laboratory analysis were carried out at the Department of Clinical Pathology & Immunology, Ain Shams University Hospital.

Histological study

The right kidney of each animal was carefully dissected and processed for light microscopic preparations. The kidneys were fixed in 10% buffered formalin solution and then paraffin blocks were prepared. Sections of 4 μm thickness were obtained and stained with

1. Haematoxylin and eosin (H&E) stain was used to examine the overall structures [39].

2. Masson's trichrome stain for identification of collagen fibers [39].

3. Periodic acid Schiff (PAS) reaction to assess the brush border of proximal convoluted tubules and to assess glomerular integrity [40].

4. Gordon and Sweet's silver impregnation staining method for identification of reticular fibers [41].

5. Immuno-histochemical staining for caspase-3 (a marker of apoptosis): four micrometer thick sections from all groups, were cut on positively charged slides and were processed using immunohistochemistry. After deparaffinization and rehydration, the sections were incubated with methanol to inhibit endogenous peroxidase activity. A citrate buffer (pH 6.0) was used to pre-treat the sections in a microwave. Room temperature incubation with monoclonal anti-caspase-3 primary antibodies (cat. MBS712464, MyBioSource, Inc. San Diego, USA) (1:200) was performed on the sections. Following the addition of streptavidin peroxidase, biotinylated goat anti-polyvalent secondary antibody, and diamminobenzidine (DAB) with chromogen to the sections, the incubation process was completed. A counterstain of Mayer's haematoxylin was applied to the slides. To create the negative control sections, the primary antibodies were not included [42]. Positive control section was done using a section of the tonsil. Positive caspase-3 reaction was seen as brown cytoplasmic and nuclear reaction. Under a light microscope, the slides were examined to determine the level of cell immunopositivity.

Histomorphometric Study:

Examination, analysis, and morphometric studies of the stained kidney sections were done using light microscopy (Lecia ICC50 W) and Leica Q Win plus Image Analysis System (Leica Micros Imaging Solutions Ltd, Cambridge, UK). Five fields from five non-overlapping randomly chosen fields per section at 400x magnification were quantified in six different rats in each group for:

- Histopathologic scoring was made according to ***Özden et al.***, [43]. The slides were coded to prevent observer bias during the evaluation. Sections were examined blindly under a light microscope by a histopathologist unaware of the treatments given. The following parameters were used to decide the degree of tubular damage, glomerular damage, and interstitial damage: Tubular dilation, tubular cast formation, tubular epithelial cell change, glomerular damage (fibrosis, atrophy, thrombosis), interstitial fibrosis, interstitial congestion/haemorrhage, and interstitial mononuclear inflammatory cell infiltration. Each parameter was determined. Results were scored from zero to three as negative (0), weakly positive (1), moderately positive (2), and strongly positive (3) for histological evaluation.

- The mean area percentage of collagen fiber content in sections stained with Masson's trichrome stain was used to assess tubulointerstitial fibrosis.

- Mesangial areas were quantified in PAS-stained tissues to assess glomerulosclerosis. The data was subsequently imported into Excel to determine percentage of the mesangial area relative to the glomerulus area [44].

- The mean area percentage of reticular fibers in Gordon and Sweet's silver impregnation stain.

- The mean area percentage of caspase-3 immunopositive reaction to assess apoptotic cells.

Statistical Analysis:

The biochemical and histomorphometric measurements were expressed as means ± standard error of the mean (SEM) and were analysed using SPSS software version 26 (SPSS Inc., Chicago, IL, USA), then compared by one-way analysis of variance (ANOVA) test then Tukey's test was done for comparison between different groups and control group. The difference was considered statistically significant if the probability value (*P value*) <0.05.

RESULTS

Results of Measuring the Body and Kidney Weights

There was significant ($P < 0.0001$) body weight loss in rats of NODAT rat model (G4), vorinostat-treated rats (G5), and metformin-treated group (G6) compared to the negative control group (G1) with more weight loss in the tacrolimus induced NODAT rat model at the end of the experiment (week 4). Interestingly, rats in G4 (NODAT rat model) exhibited significant ($P<0.0001$) decreases in body weight at week 4 versus rats in the same group at the beginning of the experiment (week 0). Rats in vorinostat treated group (G5) showed significantly ($P < 0.0001$, $P< 0.0001$; respectively) lesser weight loss compared to the NODAT model group and metformin-treated group (G6). Interestingly, rats in G6 exhibited a significant ($P < 0.0001$) increase in body weight as compared to G5. Moreover, rats in G5 exhibited an increase in body weight at the end of the experiment (week 4) but non-significant ($P=0.0950$) versus at the beginning of the experiment (week 0) (Table 1, Figure 1a).

Table 1 and Figure 1b &c showed the effect of vorinostat and metformin on the NODAT rat model regarding kidney weight (gm) and relative kidney weight to the body weight (%). Rats in G5 had a significant reduction in kidney weight ($P < 0.0001$, $P < 0.0001$; respectively), that increased with tacrolimus in the induced NODAT rat model.

Results of glycaemic parameters:

Porrini et al. [45] reported that rats were considered diabetic when FBG level ≥126 mg/dL or glycemia at 120 min (IPGTT) ≥200 mg/dL. In addition, pre-diabetes conditions occurred if FBG level ≥100 and <126 mg/dL or glycemia at 120 min (IPGTT) ≥ 140 and <200 mg/dL. There was no significant ($P >0.9999$) difference in the level of FBG between the experimental (G4, G5, and G6) and control groups (G1, G2, and G3) at week 0 (basal). However, there was a noticeable difference between the groups by week 4. Table 1 and Figure 1d indicate that the rats administered tacrolimus to establish the NODAT rat model had significantly elevated FBG levels ($P < 0.0001$) vs to the control groups (G1, G2, and G3), the vorinostat-treated group (G5), and the metformin treatment group (G6).

In the current study, according to the IPGTT, the NODAT model group showed diabetes (120-min glucose ≥200 mg/dL). Interestingly, rats in G6 developed prediabetes at the end of the experiment (week 4) at 120 min but still demonstrated a significant ($P<0.0001$) reduction in comparison to the NODAT model group. Moreover, rats in G5 exhibited a significant ($P<0.0001$) decrease in IPGTT at 120 min compared to the NODAT model group and metformin-treated group (G6) (Table 1, Figure 1e).

At week 4, the plasma insulin concentration in the NODAT rat model was significantly ($P < 0.0001$) decreased in comparison to control groups (G1, G2, G3). Also, there was a significant ($P < 0.0001$, P= 0.0416; respectively) reduction in plasma insulin concentration in the NODAT model vs G5 and G6. The level of plasma insulin concentration was significantly ($P < 0.0001$) enhanced in G5 vs G6. However, the level of plasma insulin concentration was significantly increased in G6 compared to G4 but still significantly ($P<0.0001$) decreased compared to control groups. There was no significant difference between vorinostat treated group (G5) and control groups (G1, G2, and G3) in the plasma insulin concentration ($P = 0.1040$, $P=0.0664$, and $P= 0.0600$; respectively), indicating that starting treatment with vorinostat ameliorated the effect of tacrolimus on plasma insulin concentration (Table 1, Figure 1f).

Table 1: Body weight changes, Kidney weight changes, Kidney Body weight ratio, glycaemic parameters, and biochemical parameters in all experimental groups. Data are expressed as mean ± standard error of the mean (SEM).

	G1 (negative control)	G2 (vorinostat)	G3 (metformin)	G4 (NODAT rat model)	G5 (vorinostat + NODAT model)	G6 (metformin + NODAT model)
Number of rats	6	6	6	6	6	6
Body Weight (gm)						
Week 0	236.5± 2.18	236.66±1.35	239.83±1.83	235.00±2.89	234.83± 2.92	235.00± 2.30
Week 4	258.83±2.71	255.17±0.99	255.00±1.12	188.61±3.95	240.73± 3.47	205.88± 1.71
Kidney weight (gm)						
Week 4	1.665± 0.08	1.743± 0.09	1.715± 0.10	7.342± 0.25	2.467± 0.11	5.197± 0.19
Kidney Body weight ratio (%)						
Week 4	0.642±0.028	0.683±0.035	0.672±0.041	3.905±0.174	1.024± 0.045	2.521± 0.073
Glycemia parameters						
Fasting blood glucose level (mg/dL)						
Week 0	93.66± 2.10	93.33± 1.80	93.33± 1.96	93.83± 1.88	94.00± 1.98	94.16± 1.77
Week 4	96.50±1.54	96.50± 1.54	95.16± 1.85	246.50 ± 5.37	122.83± 0.94	142.50± 2.81
Intraperitoneal Glucose Tolerance Test (IPGTT) Glucose concentración (mg/dL)						
0	114.33±0.21	114.83±0.37	115.00±0.36	226.66±1.66	137.50±1.99	175.83± 2.38
15 min	143.66±1.17	144.50±0.92	147.00±2.06	247.00±0.63	146.66±1.66	190.83± 1.53
30min	174.33±1.47	175.00±1.21	174.33±1.47	325.00±1.82	177.66±0.91	230.83± 0.83
60min	165.66±0.42	161.16±1.83	160.66±2.27	307.66±0.76	167.33±0.76	224.66± 0.33
120min	115.66±0.42	114.66±0.81	115.50±0.50	300.83±0.83	127.50±1.99	221.16± 0.54
Insulin (ng/mL)						
Week 0	0.25±0.008	0.256±0.003	0.289±0.013	0.269±0.003	0.289±0.011	0.256±0.003
Week 4	0.25± 0.006	0.25± 0.003	0.2565± 0.01	0.089±0.001	0.289± 0.01	0.123±0.005
Biochemical parameters						
Renal function						
Serum urea(mg/dl)	35.33±0.42	36.17±0.70	36.00±0.57	61.00±3.69	37.00±0.85	45.17±0.74
Serum creatinine (mg/dl)	1.287±0.017	1.287±0.015	1.282±0.011	1.90±0.03	1.36±0.02	1.63±0.02
Oxidative stress markers in renal tissue						
Malondialdehyde (MDA) nmol/mg	0.60±0.07	0.70±0.07	0.70±0.06	7.74±0.28	1.17±0.10	4.41±0.11
Total antioxidant capacity (TAC; mμ/mg)	1.32±0.04	1.33±0.03	1.345±0.041	0.60±0.02	1.157±0.06	0.90±0.02

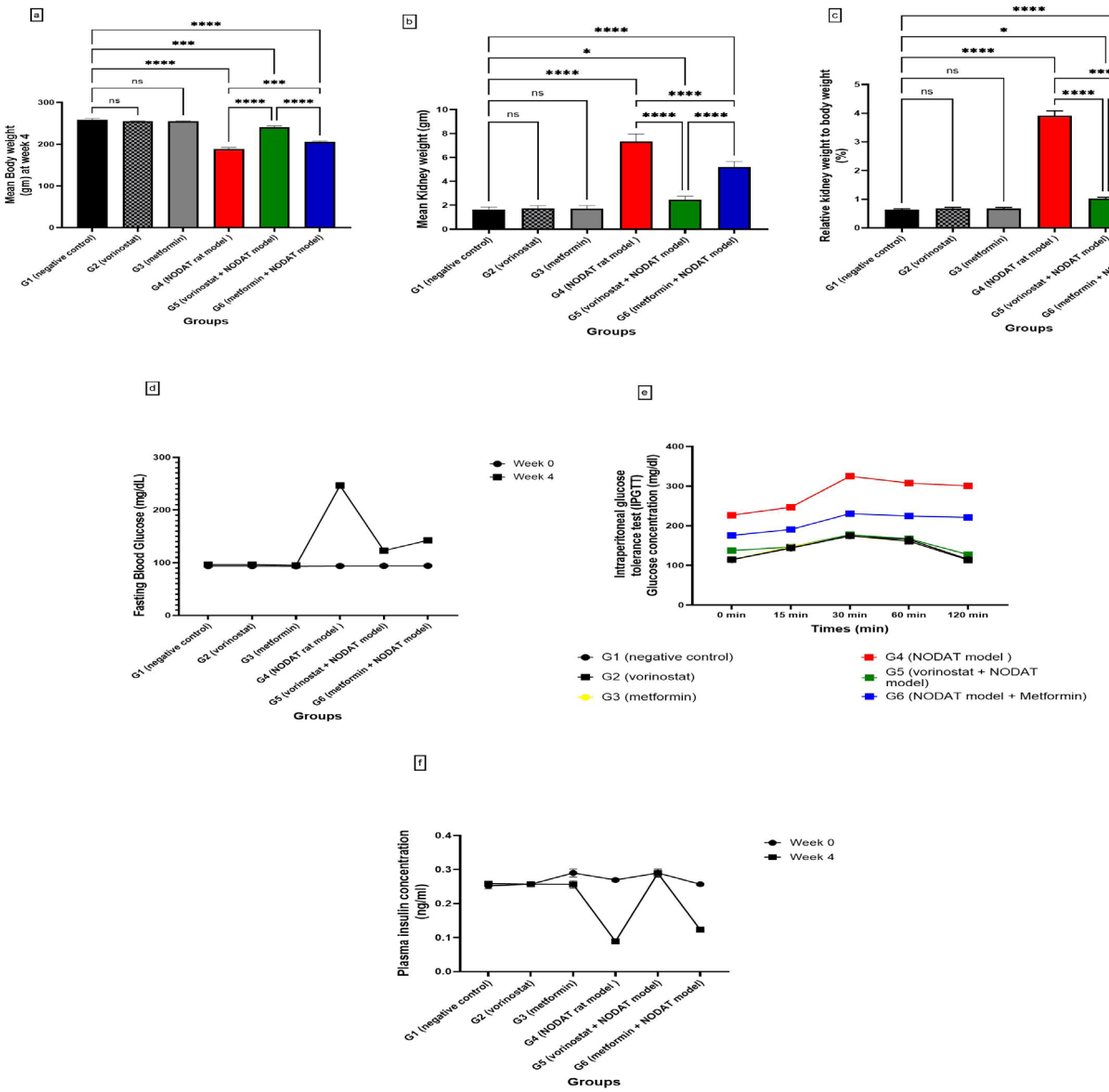

Fig. 1: Evolution of glycemia parameters in different experimental groups (a) Mean body weight (gm) at week 4, (b) Mean kidney weight (gm), and (c) Relative kidney weight to body weight (%), (d) Fasting blood glucose concentration (mg/dl), (e) Intraperitoneal glucose tolerance test (IPGTT) blood glucose level (mg/dl), and (f) Plasma insulin level (ng/ml). Data are presented as mean ± standard error of the mean (SEM). ns: not-significant, **P*<0.05, *** *P*<0.001, **** *P*<0.0001.

Biochemical results

1. Renal function test

The normal reference value of serum creatinine is 1.24 - 1.37 mg/dl and serum urea is 33.1- 40.27 mg/dl in albino rats [46,47]. The results of the current study revealed that there was a significant ($P < 0.0001$) increase in serum creatinine and serum urea levels in the NODAT rat model (G4) compared to control groups (G1, G2, G3). Moreover, there was a substantial ($P < 0.0001$) elevation in serum creatinine and urea concentrations in the NODAT rat model relative to G5 and G6. Serum creatinine and urea levels were considerably reduced ($P < 0.0001$) in G5 compared to G6. Nonetheless, blood creatinine and urea levels were markedly reduced in the metformin-treated group compared to the NODAT model, although it remains considerably elevated relative to the control groups. No significant difference was observed between vorinostat and the negative control group regarding serum creatinine and urea levels ($P = 0.2211$ and $P > 0.9999$, respectively), suggesting that initiating treatment with vorinostat mitigated the impact of tacrolimus on renal function, evidenced by a reduction in both serum creatinine and urea levels (Table 1, Figures 2 a&b).

2. Effect on oxidative stress markers.

There was a significant ($P < 0.0001$) increase of MDA level in the NODAT rat model (G4) vs the control

groups (G1, G2, G3). Also, there was a significant ($P < 0.0001$) increase of MDA level in the NODAT rat model compared to G5 and G6. The MDA level was dramatically ($P < 0.0001$) reduced in G5 relative to G6. However, the level of MDA was significantly lower in G6 compared to G4 but still significantly increased compared to control groups. There was no significant difference between G5 and control groups in the level of MDA ($P = 0.1149$), indicating that starting treatment with vorinostat as a preventive dose ameliorated the effect of tacrolimus on oxidative stress marker in the form of decreasing MDA level in renal tissue homogenate (Table 1, Figure 2c).

A substantial drop in TAC level ($P < 0.0001$) was seen in the NODAT rat model (G4) relative to the control groups (G1, G2, G3). Furthermore, there was a substantial ($P < 0.0001$) reduction in TAC levels in the NODAT model as when compared with G5 and G6. The TAC level was considerably elevated ($P < 0.0001$) in G5 relative to G6. However, the level of TAC was significantly increased in G6 compared to the NODAT model but still significantly decreased compared to control groups (G1, G2, G3). There was no significant difference between the G5 and the negative control group in the TAC level ($P = 0.1502$), indicating that starting treatment with vorinostat ameliorated the effect of tacrolimus on the TAC level in renal tissue homogenate (Table 1, Figure 2d).

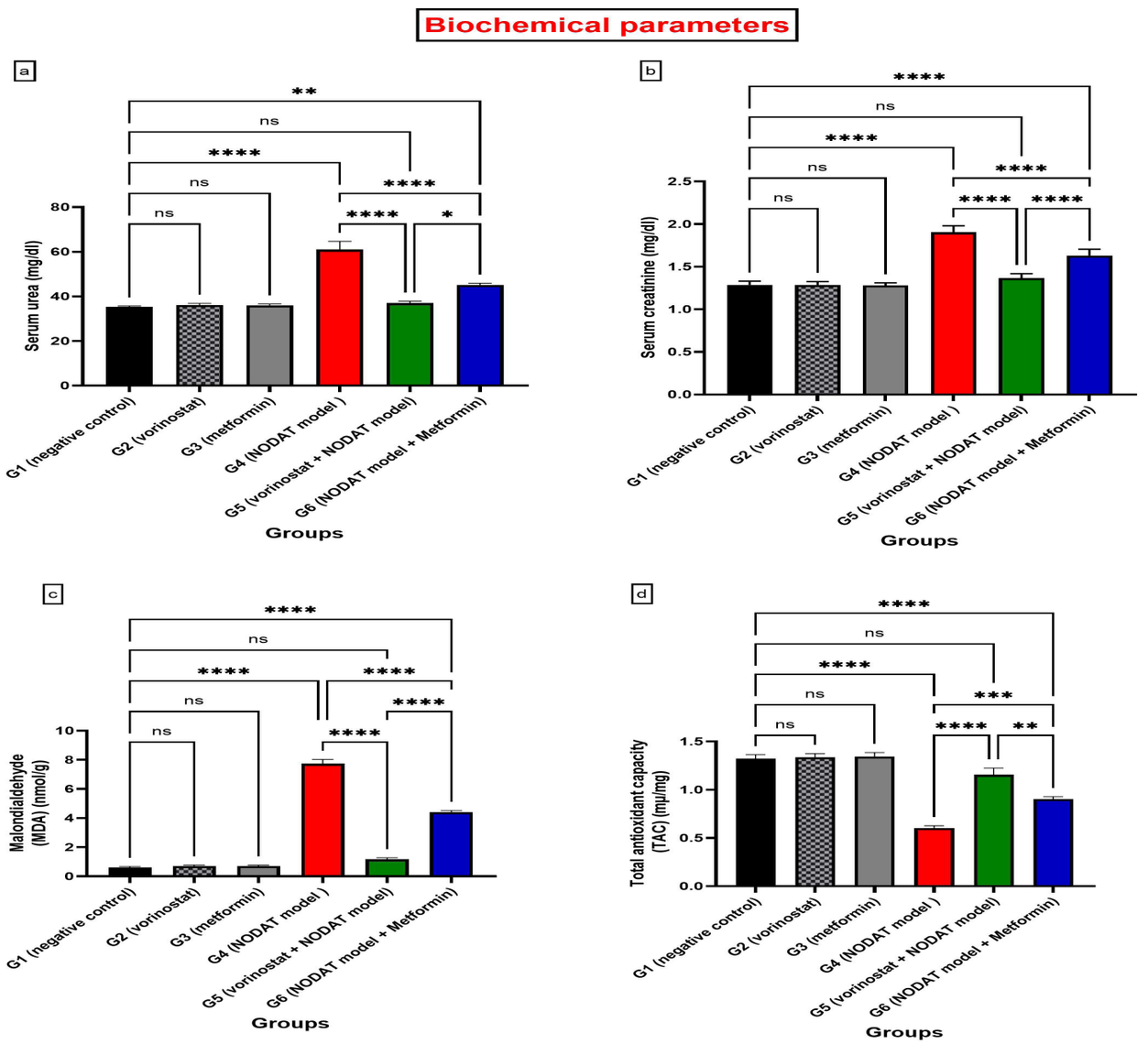

Fig. 2: Evolution of Biochemical parameters in different experimental groups renal function test in serum (a) Serum urea (mg/dl), (b) Serum Creatinine (md/dl), and oxidative stress markers in renal tissue homogenate (c) Malondialdehyde (MDA; nmol/mg) levels, and (d) Total antioxidant capacity (TAC; mμ/mg) levels. Data are presented as mean ± standard error of the mean (SEM). ns: not-significant, *P<0.05, ** P<0.01, *** P<0.001, **** P<0.0001.

Histological results:

1. Morphological evaluation of renal tissue

Haematoxylin and Eosin-stained sections

Results of control subgroups (G1a and G1b) showed similar histological, immunohistochemical and histomorphometric results in all measured parameters. They were designated as the control group. Light microscopic examination of the haematoxylin and eosin-stained sections showed normal renal corpuscles and renal tubules in the Kidney sections of the G1, G2, and G3. The renal cortices are composed of renal corpuscles, proximal and distal convoluted tubules, and the interstitial tissues. Each renal corpuscle was formed of Bowman's capsule, which included visceral and parietal layers as well as Bowman's space in the middle, and included a glomerular tuft of capillaries. The parietal layer of epithelial cells coated the other side of Bowman's capsule. The visceral layer of epithelial cells, known as podocytes, bordered the glomerular aspect of Bowman's space. Proximal and distal convoluted tubules were lined by simple cuboidal epithelium with central rounded pale basophilic nuclei. The lumina of the proximal convoluted tubules were narrower than the distal ones. The interstitial tissues contained interstitial cells with basophilic nuclei and blood vessels (Figure 3 a-c).

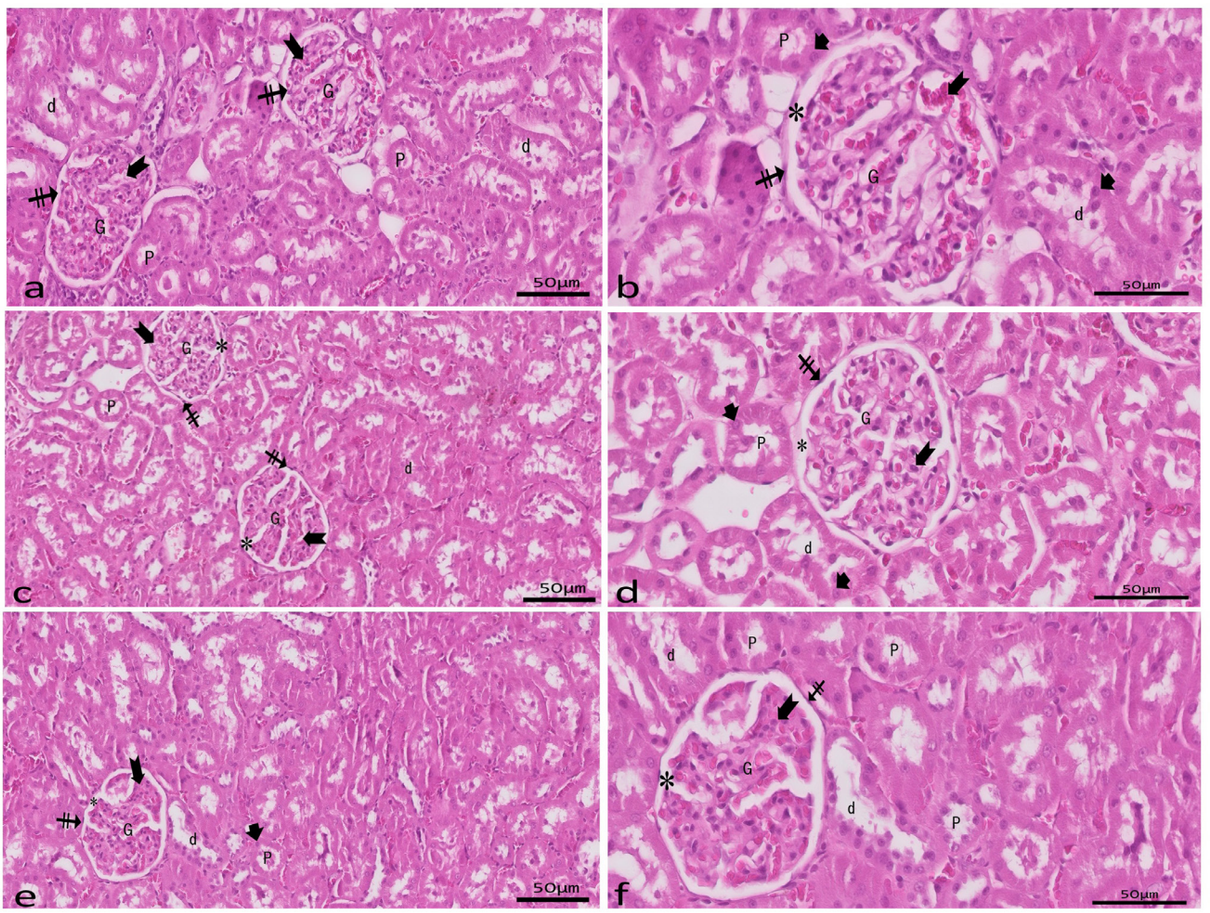

Fig. 3: H&E-stained sections in the renal cortex of: [a&b]: group 1 (G1, negative control group), [c&d]: group 2 (G2, vorinostat), and [e&f]: group 3 (G3, metformin control) showing renal corpuscles (G) each consists of glomerulus tuft (bifid arrow) surrounded by Bowman's capsule parietal layers (crossed arrow), enclosing the Bowman's space (*). Renal proximal (P) and distal (d) convoluted tubules are lined by simple cuboidal epithelium with central rounded pale basophilic nuclei (arrowhead) (H&E a, c, e x200, b, d, f x400).

H&E-stained sections in the renal cortex of NODAT model (G4, tacrolimus) demonstrated marked distortion of normal renal cortical architecture. There were some atrophied glomerular tufts with wide Bowman's space, distorted glomerular basement membrane, and other renal corpuscles with marked glomerular hypertrophy and mesangial expansion. The convoluted tubules exhibited marked distortion and degeneration of their epithelial lining with extravasation of RBCs. The proximal and distal convoluted tubules were altered in various ways, including dilatation of their lumina, thinning of their lining cells which contain darkly stained pyknotic nuclei, and cytoplasmic vacuolation. Noted areas with distorted arrangement of the convoluted tubules and with loss of epithelial lining and rarefaction of some epithelial lining with ghost nuclei were noticed. Also, there was homogenous acidophilic material in the lumen of some tubules. There was peritubular extravasation of RBCs, inflammatory cells infiltration, and dilated thick-walled congested blood vessels in the interstitium (Figure 4 a&b).

Interestingly, the renal cortex of vorinostat-treated rats (G5) displayed restoration of histological architecture compared to the control group. H&E-stained sections revealed the well-preserved structural configuration of the renal corpuscles with glomeruli surrounded by glomerular basement membrane, enclosing the Bowman's space. Notice the well-preserved structural configuration of the most proximal and the distal convoluted tubules. The lining cells of the proximal and the distal convoluted tubules were cuboidal with eosinophilic cytoplasm and vesicular nuclei. Some of the convoluted tubules showed homogenous acidophilic material in the lumen. Notice small areas of extravasation of RBCs and small blood vessels were seen in the interstitium (Figure 4 c&d).

In contrast, light microscopic examination of the H&E-stained sections of the renal cortex of metformin-treated group (G6) rats showed that most renal corpuscles and renal tubules appeared with marked degenerative changes. Inflammatory cells, extravasated RBCs, and enlarged, clogged blood vessels were seen in most interstitial tissue locations compared to the control group (Figure 4 e-f). The data clearly demonstrated that the selective metformin markedly attenuates the glomerular injury, whereas vorinostat treatment lessens the mesangial expansion but not tubular injury. The impact of vorinostat compared to metformin on the histological scoring of the kidney across various experimental groups is illustrated in (Figure 4g and Table 2).

Table 2: Histomorphometry results in all experimental groups. Data are expressed as mean ± standard error of the mean (SEM).

	G1 (negative control)	G2 (vorinostat)	G3 (metformin)	G4 (NODAT model)	G5 (vorinostat + NODAT model)	G6 (NODAT model + metformin)
Number of rats	6	6	6	6	6	6
Mean area percentage of collagen fiber (%)	9.18±0.32	9.83± 0.21	9.30± 0.51	47.22±1.54	11.73±0.34	35.32± 1.73
Mesangial areas (% of glomerulos)	90.56±0.35	81.85±4.80	90.19±0.51	45.76±6.04	82.18±4.61	50.00±6.45
Mean area percentage of Reticular fibers (%)	18.17±0.55	19.33±0.16	18.63±0.31	64.72±1.52	20.89±0.61	55.32±2.05
Area percentage of Capase-3 positive immunoreaction (%)	10.33±0.42	10.17±0.40	11.00±0.36	74.17±2.18	18.83±1.30	56.50±1.52

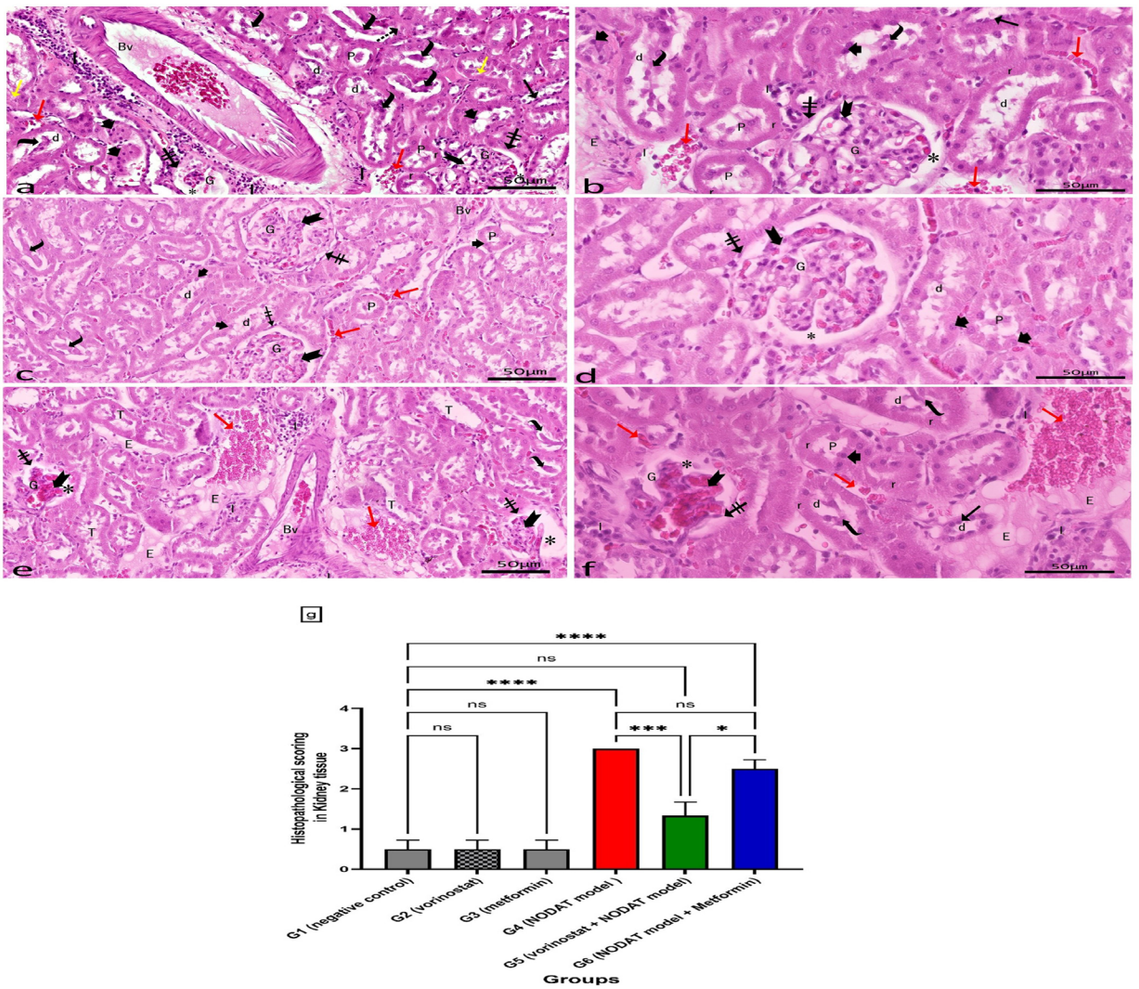

Fig. 4: (a-b): H&E-stained sections in the renal cortex of NODAT rat model group (G4) showing marked progressive glomerular and tubular damage in the form of marked glomerular (G) hypertrophy and mesangial expansion (Bifid arrow) with wide Bowman's space (*) and some glomerular tufts (G) are seen. Notice distorted parietal layer of Bowman's capsule (crossed arrow) are seen. Highly distorted and degenerated cells of the distal (d) and proximal (P) convoluted tubules which are surrounded by marked extravasated RBCs (red arrow), homogenous acidophilic material with exfoliated cells (curved arrow) in lumina of some renal tubules, most distal (d) tubules are dilated, their cells have pyknotic nuclei (arrowhead), vacuolated cytoplasm (yellow arow), and with loss of epithelial lining (dot arrow). Notice rarefaction (r) of some of the epithelial lining of the tubules, and thinning (black ↑) of the wall of some tubules are seen. Most areas of the interstitial tissues are infiltrated by inflammatory cells (I), extravasated RBCs (red arrow), oedematous eosinophilic structures (E), and dilated thickened congested blood vessel (Bv) as compared to the control. (c-d) Vorinostat-treated group (G5, vorinostat + tacrolimus) showing apparently normal histological structure of renal corpuscles with well-formed capillary tufts (bifid arrow) in glomeruli (G) and surrounded by a parietal layer of Bowman's capsule (crossed arrow) enclosing the Bowman's space (*). Renal proximal (P) and distal (d) convoluted tubules were nearly normal with vesicular nuclei (arrowhead). Some convoluted tubules show homogenous acidophilic material in the lumen (curved arrow). Notice small areas of extravasation of RBCs (red arrow) and small blood vessels (Bv) are seen in the interstitium. (e-f) Metformin-treated group (G6, tacrolimus + Metformin) showing that most of the renal corpuscles (G) and renal tubules (T) appear with marked degenerative changes. The parietal layer of Bowman's capsule (crossed arrow) is apparently thick in certain areas and in others were disrupted and discontinued, the Bowman's space (*) is wide and irregular, and the renal glomerulus (G) is shrunken with congested capillaries tuft (bifid arrow) are seen. Many proximal (P) and distal (d) convoluted tubules were hardly differentiated. Some tubular (T) cells show homogenous acidophilic material in their lumens (curved arrow). Other tubular cells have nuclei (r) with fading of their basophilia and shrunken deeply stained nuclei (arrowhead). Most areas of the interstitial tissues are infiltrated by inflammatory cells (I), extravasated RBCs (red arrow), oedematous eosinophilic structures (E), and dilated thickened congested blood vessel (Bv) as compared to the control group (H&E a, c, e x200, b, d, f x400). (g): Histological score for all groups. Results were scored from zero to three as negative (0), weakly positive (1), moderately positive (2), and strongly positive (3). ns: not-significant. *P<0.05, *** P<0.001, **** P<0.0001.

Periodic Acid Schiff (PAS) stained sections.

The renal cortex of the negative control group (G1), vorinostat group (G2), and metformin group (G3) showed a PAS-positive reaction (magenta red) in the basement membranes of the renal corpuscles, within the glomerular tufts, and the basement membranes of convoluted tubules as well as brush borders of proximal tubules (Figure 5a-c). The NODAT rat model (G4) showed a strong magenta-red reaction compared to the control group. This reaction manifested as increased PAS reaction within renal glomeruli and thickened basement glomerular membranes, parietal layer of Bowman's capsule, and most convoluted tubules. In addition, focal loss of the apical brush border

was reported of most of the convoluted tubules. Noted areas of complete loss of reaction were detected in other tubules and the basement membrane of convoluted tubules. Areas of PAS-positive hyaline casts in the tubular lumina, in the interstitial tissue, and arteriolar hyalinosis were seen (Figure 5d). Furthermore, when compared to the control group, the G5 group that received the protective dose of vorinostat seemed to have maintained the thickness of the blood vessel wall, the brush borders of the proximal convoluted tubules, and the basement membranes of the renal tubules and glomerular capillaries (Figure 5e). A strong magenta-red reaction was observed in the convoluted tubules, the parietal layer of Bowman's capsule, and increased PAS rection in renal glomeruli with thickened glomerular basement membranes in rats from group 6 (G6), which were treated with metformin. There was arteriolar hyalinosis and a bright magenta-red PAS-positive stain in the interstitial tissue (Figure 5f). The effect of vorinostat in contrast to metformin on the mesangial areas (% of glomerulus) of the kidney in different experimental groups was shown in (Figure 5g and Table 2).

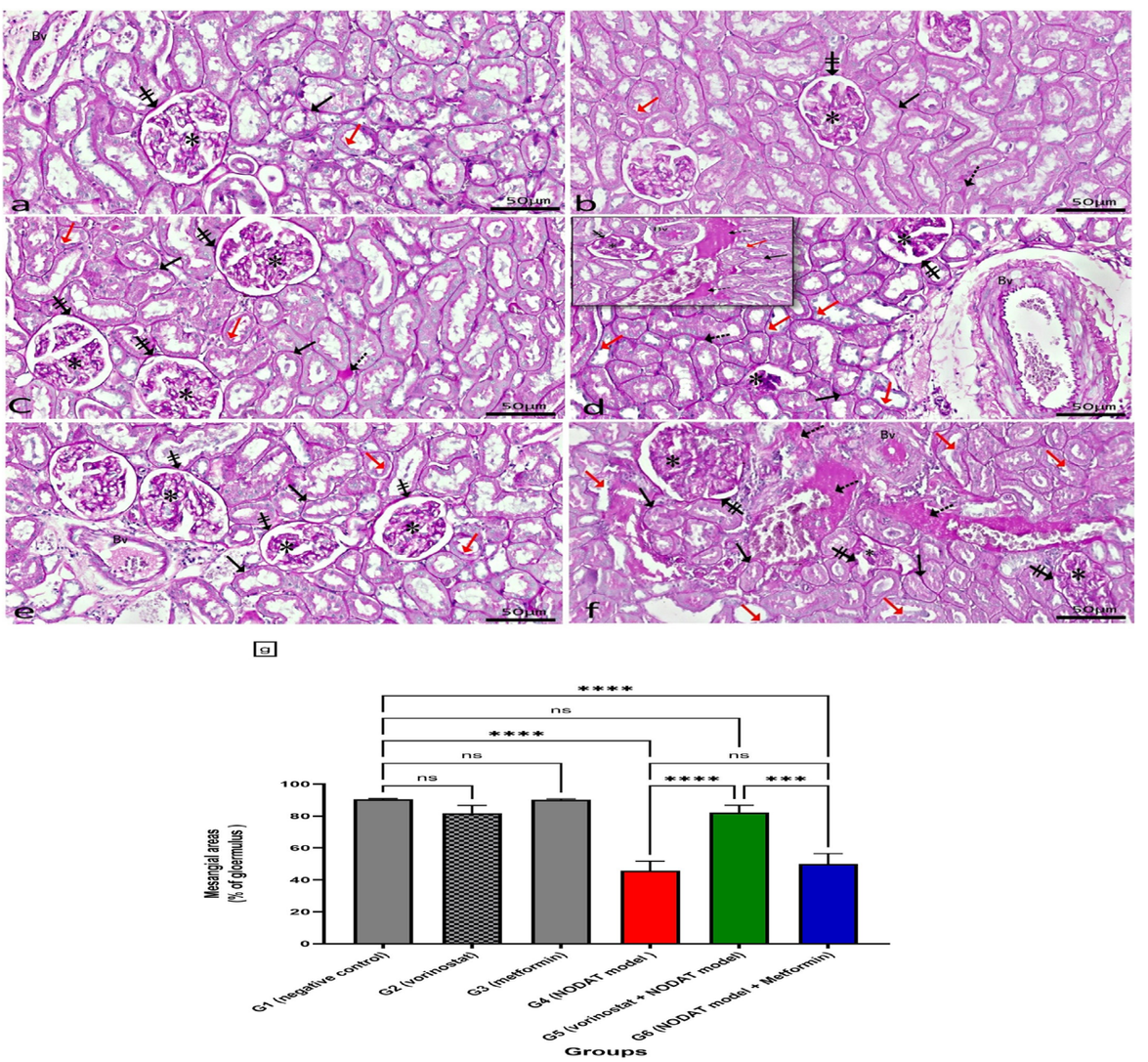

Fig. 5: Photomicrographs of PAS-stained sections of the renal cortex of (a) control group (G1), (b) vorinostat group (G2), and (c) metformin group (G3) showing PAS +ve magenta red reaction in the basement membranes of the renal corpuscles (crossed arrow), basement membranes of glomerular capillaries (*), and the basement membranes of convoluted tubules (black ↑) as well as brush borders of proximal tubules (red ↑). Notice thin wall blood vessels (Bv) and thin interstitial tissue (dashed arrow) are seen. (d) NODAT rat model (G4) showing marked loss of PAS-positive magenta red reaction in the brush borders of proximal tubules (red ↑), marked thickened tubular basement membrane (black ↑), marked thickened basement membranes of the renal corpuscles (crossed arrow), and basement membranes of glomerular capillaries (*). Notice arteriolar hyalinosis (Bv) and large areas with PAS-positive magenta red in the interstitial tissue (dashed arrow). (e) Vorinostat-treated rats (G5) apparently retain the thickness of the basement membranes of glomerular capillaries (*), parietal layer of Bowman ′s capsule (crossed arrow) and basement membranes of the renal tubules (black arrow) as compared to the control group. The brush borders (red ↑) of the proximal convoluted tubules are also restored. (f) Metformin-treated rats (G6) showing strong magenta-red reaction in the renal glomeruli (*), parietal layer of Bowman′s capsule (crossed arrow), and the convoluted tubules (black ↑). Loss of PAS reaction in the brush borders of proximal tubules (red ↑) are noticed. Notice strong PAS-positive magenta red in the interstitial tissue (dashed arrow) and arteriolar hyalinosis (Bv) are seen (PAS stain a-f x200). (g): Mesangial areas (% of glomerulus). Data are presented as mean ± standard error of the mean (SEM). ns: not-significant, *** P<0.001, **** P<0.0001.

2. Evaluation of renal fibrosis

Masson's trichrome stained-stained section

The renal cortex of the control group (G1), vorinostat group (G2), and metformin group (G3) exhibited few collagen fibers peri glomerular, peritubular, and in the interstitium surrounding blood vessels. Increased collagen fibers were found in the renal cortex of the NODAT rat model (G4), fibrotic and extravasated RBCs in the cortex acquired blue and red coloration; respectively. Also, increased collagen fibres and extravasated RBCs were demonstrated in the renal cortex tissue of metformin-treated rats (G6). In contrast, vorinostat-treated rats (G5) exhibited moderate collagen fibers deposition peri glomerular, peritubular, and in the interstitium surrounding blood vessels (Figure 6 a-f). Effect of vorinostat in contrast to metformin on the area percentage of collagen fibers in Masson trichrome stain of the kidney in different experimental groups were shown in (Figure 6g and Table 2).

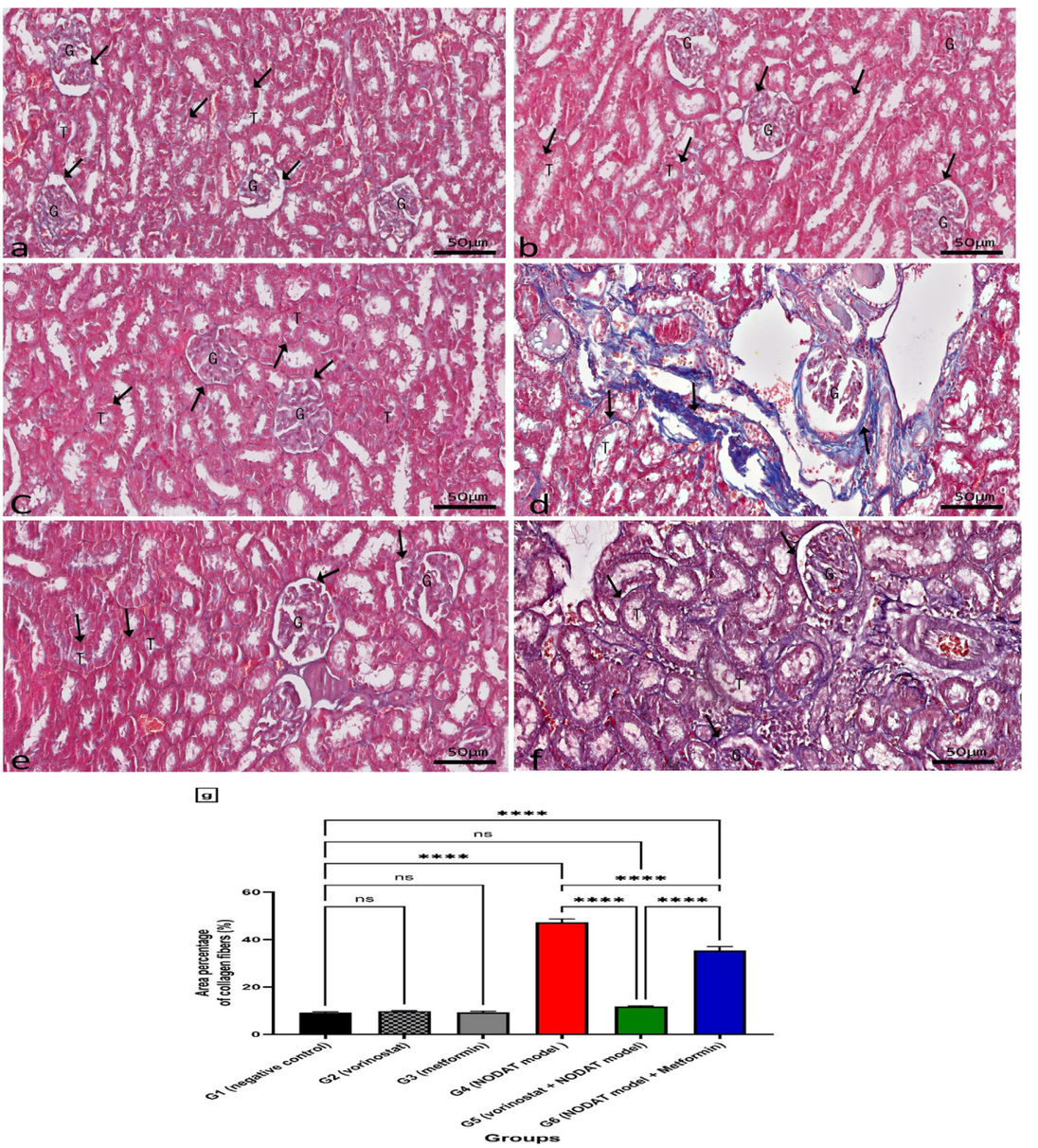

Fig. 6: Photomicrographs of Masson's trichrome stained-stained sections of the renal cortex of (a) control group (G1), (b) vorinostat group (G2), and (c) metformin group (G3) showing few collagen fibers (↑) peri glomerular (G) peritubular (T), and in the renal interstitium surrounding blood vessels (Bv). (d) NODAT model (G4) showing increased collagen (↑) fibers surrounding renal glomeruli (G) and tubules (T), and in the interstitium surrounding thickened dilated congested blood vessels (Bv). (e) vorinostat-treated rats (G5) showing collagen fibers (black arrow) around renal glomeruli (G), peritubular (T), and in the interstitium surrounding blood vessels (Bv). (f) metformin-treated rats (G6): moderate collagen fibers (↑) deposition is found per glomerular (G), peritubular (T), and in the interstitium surrounding thickened dilated congested blood vessels (Bv) (Masson's trichrome stain x 200). (g): Mean area percentage of collagen fibers. Data are presented as mean ± standard error of the mean (SEM). ns: not-significant, **** P<0.0001.

Gordon and Sweet's silver impregnation-stained sections

Gordon and Sweet's silver impregnation revealed the demonstration of reticular fibers in a section of the renal cortex of the experimental groups. The renal cortex of the control group (G1), vorinostat group (G2), and metformin group (G3) showed thin fine black stained reticular fibres supporting walls of the blood vessel, the glomeruli, the tubular basement membrane, and in the peri-tubule-interstitial tissue. The kidney sections of the NODAT rat model (G4) showed an apparent increase of reticular fibers supporting walls of the blood vessel, around the glomeruli, the tubular basement membrane, and in the interstitial tissue. Interestingly, vorinostat-treated rats (G5) showed reduced reticular fibres in the kidney cortex. However, metformin-treated rats (G6) exhibited dark black staining affinity in the reticular fibres, but it had still appeared increased than control (G1) and G5 (vorinostat treated group) (Figure 7 a-f). Effect of vorinostat in contrast to metformin on the area percentage of reticular fibers in Gordon and Sweet's silver impregnation stain of the kidney in different experimental groups was shown in (Figure 7g and Table 2).

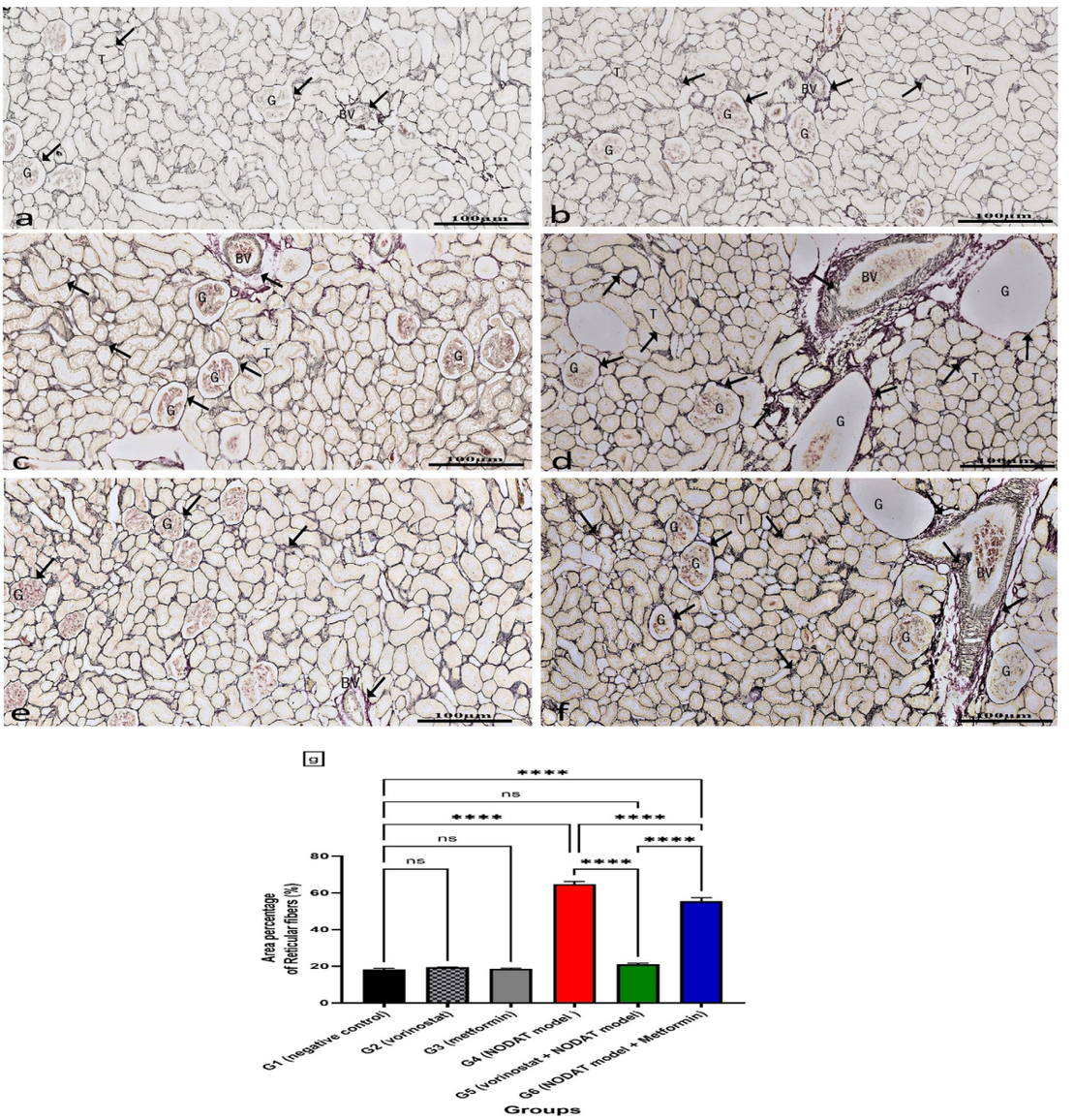

Fig. 7: Photomicrographs of Gordon and Sweet's silver impregnation staining sections of the renal cortex of (a) control group (G1), (b) vorinostat group (G2), and (c) metformin group (G3) showing fine thin black stained reticular fibers (↑) supporting walls of the blood vessel (BV), around the glomeruli (G), and in the peri-tubule-interstitial tissue (T). The renal cortex of NODAT rat model (G4) rats showing an apparent increase of the dark black staining affinity in the reticular fibers (↑) supporting walls of the blood vessel (BV), around the glomeruli (G), increased thickening of the tubular (T) basement membrane, and in the peri-tubule-interstitial tissue. Vorinostat-treated rats (G5) showing an apparent decrease in the reticular fibres (↑). However, metformin-treated rats (G6) dark black (↑) reticular fibres still appear increased than control and G5 (Gordon and Sweet's silver impregnation x 100). (g): Mean area percentage of reticular fibers. Data are presented as mean ± standard error of the mean (SEM). ns: not-significant, **** P<0.0001.

3. Evaluation of apoptosis marker (Caspase-3) expression in renal tissue

The control group (G1), vorinostat group (G2), and metformin group (G3) revealed a negative caspase-3 reaction in all renal glomeruli, renal tubules, and in the interstitial capillaries. The kidney sections of NODAT rat model rats (G4) revealed a strong positive cytoplasmic and nuclear caspase-3 reaction in the renal glomeruli, renal tubules, and in interstitial capillaries. Vorinostat-treated rats (G5) revealed the weakest caspase-3 reactions in the renal tubules, while the renal glomeruli had negative reactions. Mild nuclear caspase-3- reaction was seen in the interstitial capillaries. However, metformin-treated rats (G6) showed strong positive cytoplasmic and nuclear caspase-3 immuno reaction in renal tubules, the renal glomeruli, and in the interstitial capillaries (Figure 8 a-f). Effect of vorinostat in contrast to metformin on the area percentage of Capase-3 positive immunoreaction (%) of the kidney in different experimental groups was shown in (Figure 8g) and (Table 2).

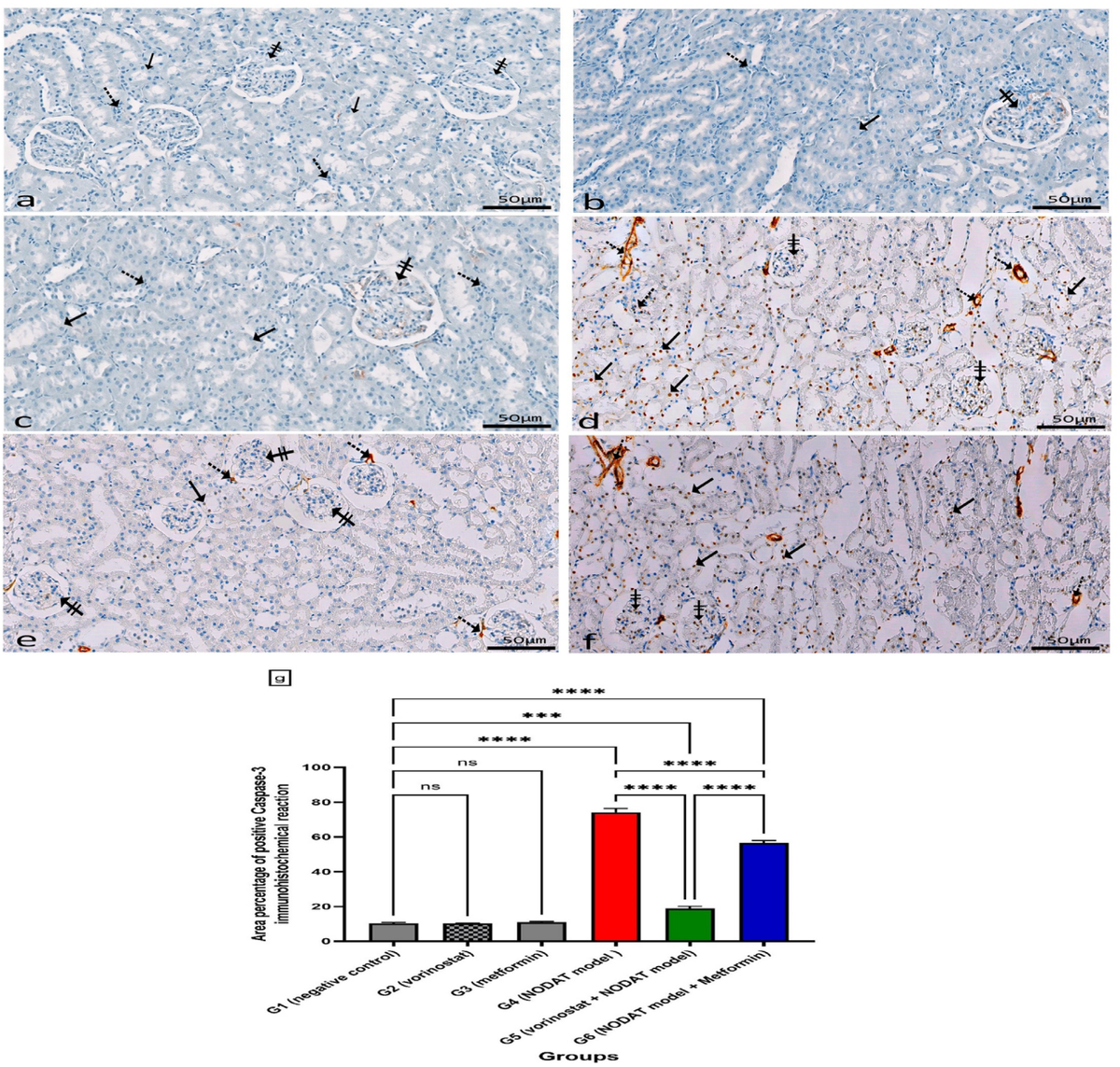

Fig. 8: Immunohistochemical staining of rats' Kidneys with anti-caspase-3 antibodies. (a) control group (G1), (b) vorinostat group (G2), and (c) metformin group (G3) reveal a negative caspase-3 reaction in all renal glomeruli (crossed arrow), renal tubules (black↑), and in the interstitial capillaries (dashed arrow). The kidney sections of (d) NODAT rat model (G4) revealing a strong cytoplasmic and nuclear caspase-3 reaction in the renal glomeruli (crossed arrow), renal tubules (black↑), and in the interstitial capillaries (dashed arrow). (e) Vorinostat-treated rats reveal weak caspase-3 reaction in the renal tubules (black↑) and negative reaction in the renal glomeruli (crossed arrow). Notice, that there is a mild weak positive caspase-3-reaction in the interstitial capillaries (dashed arrow). (F) The metformin-treated rats (G6) show a higher distribution of strong positive cytoplasmic and nuclear caspase-3 immuno reaction in renal tubules (black↑), the renal glomeruli (crossed arrow), and in the interstitial capillaries (dashed arrow) (anti-Caspase-3 immunohistochemistry x 200). (g): Mean area percentage of positive caspase-3 immunohistochemical reaction. Mean area percentage of caspase-3 immunohistochemical positive data are expressed as mean ± standard error of the mean (SEM). ns: not-significant, *** P<0.001, **** P<0.0001.

DISCUSSION

The American Diabetes Association (ADA) divides diabetes into four basic forms: type 1 diabetes, gestational diabetes mellitus, type 2 diabetes mellitus, and additional types of diabetes that are induced by specific circumstances, like new-onset diabetes after transplantation (NODAT) [48,49]. Among the several immunosuppressants used to treat transplant recipients, tacrolimus is among the most used[50]. NODAT is considered an important side effect of tacrolimus treatment [51]. Curiously, insulin sensitivity was found to increase following acute intravenous infusions of tacrolimus in a clinical trial including healthy individuals [52]. Patients given tacrolimus as their primary immunosuppressive medication had an increased risk of posttransplant diabetes mellitus (PTDM) and metabolic syndrome, according to a Spanish retrospective study[53]. Hence, immunosuppressant treatment after organ transplant was simulated in the present study using an in vivo model.

The use of insulin and oral hypoglycemic medicines to treat PTDM is fraught with clinical problems, such as the potential for these treatments to combine with other drugs required to avoid organ rejection and their negative effects[54]. Improving transplant patient outcomes and the donated organ's long-term success can be achieved with an ideal new treatment strategy that prevents PTDM without removing tacrolimus. Here, we used vorinostat as a protective treatment to avoid tacrolimus-induced hyperglycemia.

In the current study, adult male albino rats were chosen as an animal model, to avoid the effect of female hormones which may play a role in decreasing the risk of developing kidney failure relative to males [55]. In the current study, a successful NODAT rat model was performed using prolonged treatment of the rats with tacrolimus. After 14 days of tacrolimus therapy, the Wistar albino rats developed hyperglycemia and entered a diabetic condition. In a similar vein, ***Zhang et al.*** [56] found that rats given tacrolimus for 10 days acquired hyperglycemia and glucose intolerance. A recent research has concentrated on islet cell injury [57], while earlier studies demonstrated that PTDM after organ or cell transplantation can be caused by varying dosages of tacrolimus in animal models [58].

Measuring the mean body weight in the present study showed a significant decrease in the NODAT rat model compared to the control groups. This is in agreement with the results of ***Li et al.*** [59] who stated that tacrolimus-induced diabetes showed a significant reduction of body weight, ill-looking, and polydipsia in diabetic rats. ***Ewenighi et al.*** [60] demonstrated that the weight loss in diabetic rats might be due to increased glycogenolysis, lipolysis, and gluconeogenesis, leading to protein loss and muscle wasting. Because vorinostat inhibits weight gain, the G2 group of rats given the drug for four weeks had a lower body weight than the G1 and G3 control groups[30]. However, treatment of NODAT rats with vorinostat (G5) and metformin (G6) exhibited significant partial restoration of the body weight compared to the NODAT rat model and still with a considerable decrease compared to the control groups. Our findings corroborate those of prior research showing that metformin successfully mitigated the consequences of diabetes generated by Sirolimus but had no such effect on tacrolimus. Various metformin effects on diabetes appear to be associated with distinct diabetes etiologies [34]. These findings could help shed light on NODAT and guide the selection of antidiabetic medications for individuals afflicted with the condition.

A notable rise in kidney weight was noted in the NODAT rat model. Consistent with previous researches, the current study produced the same outcome [36,61]. The enlargement of the kidneys in T2DM is thought to be caused by a combination of processes, including the kidneys' increased glucose uptake, glycogen storage, lipogenesis, and protein synthesis [62]. The vorinostat effectively stopped the NODAT rats' kidneys from enlarging. Our findings corroborate those of ***Gilbert et al.*** [29], who hypothesized that smaller kidneys could be due to slower cell proliferation, higher cell death, or both. The in vivo proliferation of tubular cells was reduced in diabetic rats treated with vorinostat. Despite their ability to accelerate tumor cell death, HDAC usually exhibit exceptional selectivity, causing insignificant damage in normal cells.

The glucose tolerance test and the random evaluation of plasma glucose after 8 hours of fasting reveal glucose changes, which are linked to the progressive loss of pancreatic β-cell activity that defines T2DM [63,64]. These changes provide the foundation for identifying hyperglycemia or hyperglycemic crisis, which are the basic indications of the condition [65]. In order to determine how tacrolimus affected insulin sensitivity and glucose homeostasis, a battery of tests was conducted. The gold standard for diagnosing PTDM, the host glucose loading capacity, was evaluated using the IPGTT [59]. Week 4 glucose concentrations in tacrolimus-treated rats peaked at 325.00 mg/dL 30 minutes after intraperitoneal injection of 2 g of glucose in the glucose tolerance test (GTT), before declining somewhat to 300.83 mg/dL 120 minutes later. This results in a rightward shift of the curve, which indicates a lack of tolerance for carbohydrates. This came in accordance with ***Quintana-Pérez et al.*** [49] and ***Zhang et al.*** [56].

The secretion of insulin by pancreatic β cells leads to the entry of circulating glucose into cells when the blood glucose concentration is high (hyperglycaemia). The uptake and storage of glucose are facilitated by receptors in liver, muscle, and adipose tissue [66]. Therefore, T2DM and non-insulin-dependent atrial fibrillation begin with peripheral tissue insulin resistance and persistent hyperinsulinemia[67,68]. Pancreatic β cells gradually degenerate and finally can't keep producing an elevated level of insulin because of the

increased demand for the hormone. As a result, glucose metabolism pathways become dysfunctional due to persistent hypoinsulinemia and hyperglycemia. Diagnosis of metabolic disorders, including diabetes, relies on these altered characteristics[69,70]. According to in vivo and in vitro research, the main impact of tacrolimus on hyperglycemia is its effects on insulin secretion and synthesis [71,72].

Insulin secretion in response to glucose is impaired in rodent islets and cell lines treated with calcineurin inhibitors, according to previous researches [73–75]. As a measure of the pancreatic β cells' functional capacity, the concentration of plasma insulin was measured in this study. At week 4, the experimental animals in the NODAT model group showed significantly lower insulin levels compared to the control groups, according to the present study's results. This is in accordance with ***Tosur et al.*** [76] and ***Uchizono et al.*** [77]. ***Tosur et al.*** [76] found that pancreatic β cells had a high concentration of tacrolimus binding protein, which could explain why the experimental group had low insulin levels. It has been proposed that tacrolimus inhibits insulin granule exocytosis, a process that is involved in glucose-stimulated insulin production in rat islets, according to research by ***Uchizono et al.*** [77]. The same condition is also shown in ***Quintana-Pérez et al.*** [49].

The most important finding of this study is that vorinostat and metformin treatment for 4 weeks caused different glucose-lowering effects. Metformin improved this condition, but not to the degree seen in vorinostat. When added to tacrolimus, vorinostat reduced hyperglycemia and raised plasma insulin levels in the vorinostat group but had no such impact in the metformin group. Our findings corroborate those of prior research showing that metformin considerably decreased mean random glucose levels in rats treated with sirolimus but not tacrolimus [78].

When comparing the NODAT group to the control groups, the measurements of serum urea and creatinine showed a statistically significant rise in the former. We confirmed the findings of ***Xie et al.*** [79] that tacrolimus produces hyperglycemia, which may be associated with renal failure, damage, and elevated levels of urea, uric acid, and creatinine in the blood. Interestingly, the results of the current study showed a substantial elevation in the urea and creatinine in the metformin-treated group relative to the vorinostat-treated group (G5) and control groups. Our findings indicated that metformin was not suitable in the NODAT rat model. Consistent with this result, ***Inzucchi et al.*** [80] found that blood creatinine levels exceeded specified safety limits in 1 out of 22 (4.5%) individuals treated with metformin in general practice. This could be explained by ***Hsu et al.*** [81] who reported that the use of metformin is contraindicated in men and women with serum creatinine concentrations of 1.5 mg/dL or higher and 1.4 mg/dL or higher, respectively, due to the risk of the life-threatening complication, lactic acidosis. Impaired renal function can lead to accumulation of metformin and elevated concentrations of metformin have been associated with lactic acidosis. Researches by ***Gilbert et al.*** [29] and ***Advani et al.*** [28] found that vorinostat reduces kidney damage in rats and mice with diabetes. They found that vorinostat reduced diabetes-related kidney hypertrophy and tubule cell proliferation.

A key component in the development and progression of diabetes is oxidative stress, which occurs when the body's antioxidant defences are inadequate to deal with the excess free radicals produced by the disease [82]. Hyperglycemia is one of the causes of elevated oxidative stress [83]. It would appear that oxidative stress is a major contributor to cell death and disease [84]. One of the main causes of kidney damage in diabetic individuals is oxidative stress, which leads to lipid peroxidation and elevated levels of oxygen free radicals [85,86]. In the current work, the statistical analysis of MDA mean values sets up evidence of cell death by revealing a highly significant rise in the NODAT group and metformin-treated group compared to the other groups. ***Gao et al.*** [87] declared an increase in MDA levels in kidney tissue following the tacrolimus-induced NODAT model. According to their findings, tacrolimus can cause renal vasoconstriction, which in turn causes hypoperfusion and hypoxia-reoxygenation damage, and finally, the production of free radicals or reactive oxygen species (ROS). The direct impact of tacrolimus on ROS production is still not well understood. In this study, we found that diabetic rats treated with vorinostat had a considerable reduction in oxidative stress markers (MDA) and an increase in total antioxidant capacity (TAC) in kidney homogenates. These results support the assertions that vorinostat is a powerful antioxidant. Since MDA is a byproduct of unsaturated fatty acid lipid peroxidation, its reduction by vorinostat may be interpreted as an indicator of reduced oxidative stress and, by extension, cytotoxicity.

The “gold standard” for diabetic nephropathy diagnosis is renal histopathological changes [88]. Diabetic nephropathy is characterized by an accumulation of extracellular matrix, thickening of the glomerular basement membrane, invasion of inflammatory cells into the renal interstitial space, fibrosis of the renal interstitial space, and glomerular sclerosis [89]. The microscopic changes in the kidney in the NODAT rat model group were more obvious in the renal cortex [90], so the present study focused on the histopathological changes of the renal cortex. In the present study, histological examination of the renal sections of the NODAT rat model group revealed marked histopathological changes. H&E, Masson trichrome, PAS, and Gordon & Sweets’ silver impregnation staining demonstrated significant renal injuries, including a thickened parietal layer of Bowman’s capsule, an enlarged irregular Bowman’s space, and atrophied glomeruli. These findings were statistically validated by a substantial reduction in glomerular diameter and a marked increase in the percentage area of collagen fibers and PAS-positive reactions, alongside a substantial reduction in the area

percentage of reticular fibers relative to the control groups. Consistent with these results, ***Fu et al.*** [44] used a novel approach to study tacrolimus-induced nephropathy and renal interstitial fibrosis in rats by administering the drug for two weeks after renal ischemia-reperfusion. Tubular vacuolization, arteriolar hyalinosis, interstitial fibrosis, and juxtaglomerular hyperplasia are similar to histological and ultrastructural alterations previously documented in nephrotoxicity caused by tacrolimus [91].

In the present study, the lining cells of the proximal convoluted tubules (PCTs) in the NODAT rat model group demonstrated destruction of apical microvilli, marked vacuolation, and rarified cytoplasm with dark deeply stained pyknotic nuclei. The distal convoluted tubules (DCTs) showed complete detachment of the lining cells from their basement membrane into the lumen in some tubules. The nuclei of the cells of distal convoluted tubules were squeezed and their cytoplasm was swollen (hydropic degeneration).

The finding of the current study is following ***Donder et al.*** [92] who mentioned that there were histopathologic changes in DN including thickening of the basement membrane, as well as tubular vacuolation and mesangium proliferation. In addition, our results go in agreement with Schlo and Banas [93] who stated that there was also a thickening of the glomerular basement membrane, expansion of podocyte slit membranes, and mesangial hypertrophy in diabetic nephropathy. Tubule cell vacuolization may be a form of adaptive mechanism under a demanding condition (Diabetes) and subsequent cell disruption. It is linked to glycogen deposition and lipid vacuoles formation [94]. Diabetic patients had substantial dilatation of the distal tubules, as well as separation and tubular epithelial degradation [95].

Our results showed that diabetic rats have reduced renal function and increased kidney weight, which may indicate that glucose has a toxic effect and damages the kidneys. The hallmarks of DN, as shown on histology, include the growth of the mesangial matrix, arteriolar hyalinosis, and Armanni-Ebstein lesions (vacuolization and PAS-positive glycogen accumulation in the cytoplasm of tubular epithelial)[96]. These histological features of DN were also observed in the present study's NODAT rats. Glycogen aggregates due to enhanced tubular glucose uptake induce Armanni-Ebstein lesions, also known as vacuolization of tubular epithelia. As the filtered load increases, the proximal tubule's ability to reabsorb glucose is enhanced by the rise in plasma glucose [97]. The current research found that vorinostat significantly reduced renal structural damage and improved kidney function in diabetic rats. One may speculate that in this group, the decreased tubular glucose load may cause less glucotoxicity-related kidney injury, given that blood glucose levels were also lower after vorinostat treatment.

In the present study, a light microscopic examination of the vorinostat-treated NODAT rat model showed normal glomerulus nearly appeared as control groups. However, there were some congested capillaries. In the present study, improvement of renal tubules occurred. PCTs showed most of the cells had vesicular nuclei with a minimal amount of vacuolations. DCTs showed most of the lining cells with vesicular nuclei. All the histological results were confirmed statistically. This is in agreement with the study of ***Advani et al.*** [28] who stated that vorinostat was able to alleviate renal tissue damage of diabetic nephropathy after significant reversion of the pathological changes of kidneys in diabetic nephropathy rats. The results of the current study could be explained by ***Gilbert et al.*** who demonstrated that the HDACi, vorinostat, attenuated early renal enlargement in experimental diabetes and that this effect is likely to be mediated, at least in part, by downregulation of the epidermal growth factor receptor [29].

H&E-stained sections of the metformin-treated tacrolimus-induced NODAT rat model revealed that the most significant finding which is the marked apparent dilatation of capillaries between the renal corpuscles and renal tubules filled with erythrocytes. It was the most advanced change all over the normal renal tissue. These results paralleled with that attained by ***Adaramoye et al.***[98] who recorded that metformin hydrochloride and glibenclamide had a toxic effect on some organs of male rats. Our findings could be explained by ***Citro et al.***[99] and ***Fareed et al.***[100]. Consistently high blood sugar levels, the researchers found, lead to hyperfiltration and vasodilatation, which in turn promote structural atrophy in the glomeruli and clogged glomerular capillaries in diabetic rats[99,100]. In addition, albuminuria, endothelial dysfunction leading to increased permeability and glomerular hyperfiltration, and protein kinase C (PKC) activation are all outcomes of hyperglycemia. PKC also increases Prostaglandin (PGE1) production and activates vascular endothelial growth factor[101].

Using the Masson's trichrome stain, the present study found that in the NODAT rat model (G4) and the Metformin-treated rat model (G6), the silver impregnation examination by Gordon & Sweets revealed the breakdown of reticular fibers that formed the kidney's supporting connective tissue, the accumulation of collagen fibers in the areas where the reticular fibers were broken down, and an excess of glycogen deposition in the PAS stain. Curiously, the kidney portion of the NODAT rat model treated with vorinostat (G5) did not exhibit these histological alterations that remained in diabetic rats treated with metformin.

Some renal tubules in the NODAT rat model group showed focal loss of PAS reaction in their brush borders which was in line with ***Kidokoro et al.***[102] who reported that the glycocalyx damage is caused by tacrolimus-induced oxidative stress. During oxidative stress, the uncoupled endothelial nitric oxide synthase induces endothelial cell

dysfunction, activation, and recruitment of leukocytes and results in the denudation of the glycocalyx. Moreover, ***Fareed et al.*** [100] reported that the basement membrane of the parietal layer of Bowman's capsule and convoluted tubules of the renal cortex showed weak PAS reaction with areas of focal damage of proximal convoluted tubules brush border. This could be attributed to reactive oxygen molecule production that led to damage to cytoskeletal integrity. Our findings, together with ***Advani et al.*** [28] in other kidney disease models, showed that HDACis continues to be beneficial in diabetic nephropathy. ***Advani et al.*** [28] found that diabetic mice showed an improvement in albuminuria and mesangial matrix buildup after long-term therapy with vorinostat. This improvement was achieved through an eNOS-dependent mechanism.

Renal fibrosis is a hallmark of chronic renal disease and is defined by the excessive and persistent buildup of extracellular matrix (ECM). Renal fibrosis is mostly attributed to excess ECM, which results from an imbalance between its production and breakdown[103,104]. Renal fibrosis is characterized by an increase in the manufacture of interstitial collagens, particularly collagen IV, or a decrease in their breakdown, resulting in a thickening of the glomerular basement membrane and renal insufficiency[105]. One common way to find collagen deposition is by Masson's trichrome staining. Increased collagen fibers in NODAT model rat kidney tissues were found in the present study, suggesting that diabetes can produce renal fibrosis. Protein kinase C, mitogen-activated protein kinase, and profibrotic cytokines like TGFβ1 and VEFG are stimulated, according to ***Mohammad et al.*** [106], which leads to enhanced collagen deposition in DN. The reduction of collagen fibers in the NODAT rat model treated with vorinostat suggests that the drug may mitigate the pathophysiology of renal fibrosis in NODAT rats. Additionally, HDAC inhibitors can improve diabetic nephropathy renal lesions [107,108]. This could be explained by ***Li et al.*** [109] who reported that HDAC inhibitors caused inhibition of renal fibrosis by regulating a pathway through TGF-β. Interestingly, the results of the current study showed that metformin exhibited a significant increase in collagen fibers deposition. Our results are not in line with the previous research by ***Wang et al.*** [110] who reported that metformin has a beneficial effect on tubulointerstitial fibrosis in different stages of DN. This could be interpreted as they tested on streptozotocin (STZ)-induced DN rats not on the NODAT rat model.

One of the key mechanisms of tacrolimus-induced kidney damage is apoptosis, a form of programmed cell death[111,112]. Researches have shown that oxidative stress is a typical cause of cells dying by apoptosis. Jin and colleagues [58] have previously noted that oxidative stress caused by tacrolimus leads to cell death (both apoptotic and autophagic), which is directly linked to both structural and functional damage to the kidneys. Because of its catalytic action on numerous essential cellular proteins, caspase-3 is recognized as a crucial apoptotic mediator. The current study found that rats given tacrolimus as the only treatment for their kidneys had significantly higher levels of caspase-3 in the cytoplasm of their proximal tubular cells. The staining for caspase-3 was significantly reduced in kidneys that were collected from diabetic rats treated with vorinostat. These findings suggest that vorinostat protective effects are associated with redox status correction, inflammation abatement, and apoptosis prevention.

Our study's findings could potentially be used in the medical field. Although our study's findings support the idea that patients with NODAT should have their antidiabetic medication selection determined by the type of immunosuppressant that is producing NODAT, the existing guidelines for NODAT therapy are based on the treatment of T2DM. When it comes to managing hyperglycemia, metformin is not an appropriate antidiabetic medication for patients with tacrolimus-induced post-transplantation diabetes. Vorinostat, on the other hand, is an HDACi that may be useful because of the protection it provides against different types of damage[113]. Patients with tacrolimus-induced post-transplantation diabetes may also benefit from vorinostat, according to our findings. A more compelling case for NODAT therapy in post-transplant patients may emerge from this method.

CONCLUSION

From results of the current work, vorinostat was found to be more effective than metformin in protecting rat kidneys against in tacrolimus-induced NODAT rat model. Protective effects vorinostat was achieved by controlling hyperglycaemia, increasing antioxidant capacity, decreasing oxidative damage, halting apoptosis, and improving kidney structure and function. Therefore, vorinostat showed a double-edged sword: it prevented kidney damage and improved biochemical outcomes.

CONTRIBUTORS

The authors confirm contributions to the paper as follows: study conception and design, Dr. Heba Fikry, Dr. Lobna A. Saleh, Dr. Doaa Ramadan Sadek, Dr. Hadwa Ali Abd-Alkhalek; data collection, Dr. Heba Fikry, Dr. Lobna A. Saleh, Dr. Doaa Ramadan Sadek, Dr. Hadwa Ali Abd-Alkhalek; analysis and interpretation of results, Dr. Heba Fikry, Dr. Doaa Ramadan Sadek; manuscript draft preparation, Dr. Heba Fikry, Dr. Doaa Ramadan Sadek. All authors reviewed the results and approved the final version of the manuscript.

CONFLICT OF INTEREST

The authors declare that no funds, grants, or other support were received during the preparation of this manuscript.

REFERENCES

1. **Zielińska K, Kukulski L, Wróbel M, Przybyłowski P, Zielińska M, Strojek K.** New Onset Diabetes after Transplantation (NODAT)—scientific data review. Clin Diabetol 2020;9:356–66.

2. **Vest AR, Cherikh WS, Noreen SM, Stehlik J, Khush KK.** New-onset diabetes mellitus after adult heart transplantation and the risk of renal dysfunction or mortality. Transplantation 2022;106:178–87.

3. **Kumar S, Sanyal D, Das P, Bhattacharjee K, Rungta R.** An observational Prospective Study to Evaluate the Preoperative Risk Factors of New-onset Diabetes Mellitus after Renal Transplantation in a Tertiary Care Centre in Eastern India. Indian J Endocrinol Metab 2018;22:610–5. https://doi.org/10.4103/ijem.IJEM_121_18.

4. **Chowdhury TA.** Post-transplant diabetes mellitus. Clin Med 2019;19:392–5. https://doi.org/10.7861/clinmed.2019-0195.

5. **Kun-Ming P, Can C, Qing X, Wei W, Qian-Zhou L, Xiao-Yu L.** Calcineurin inhibitor–associated new-onset diabetes mellitus in chronic kidney disease treatment: a 4-year single-center cross-sectional study in China. Eur J Clin Pharmacol 2021;77:961–9.

6. **Penteado LAM, Lucena GM, Peixoto MOB, Barbosa TC, Arruda AC de SL, Cimões R.** Evaluation of the effect of tacrolimus on periodontitis induced in rats. Arch Oral Biol 2017;80:89–94.

7. **Chien Y-S, Chen Y-T, Chuang C-H, Cheng Y-T, Chuang F-R, Hsieh H.** Incidence and risk factors of new-onset diabetes mellitus after renal transplantation. Transplant. Proc., vol. 40, Elsevier; 2008, p. 2409–11.

8. **Lancia P, Adam de Beaumais T, Elie V, Garaix F, Fila M, Nobili F, *et al.*** Pharmacogenetics of post-transplant diabetes mellitus in children with renal transplantation treated with tacrolimus. Pediatr Nephrol 2018;33:1045–55.

9. **Noble J, Terrec F, Malvezzi P, Rostaing L.** Adverse effects of immunosuppression after liver transplantation. Best Pract Res Clin Gastroenterol 2021;54:101762.

10. **Lema-Pérez L.** Main organs involved in glucose metabolism. Sugar Intake-Risks Benefits Glob Diabetes Epidemic 2021:1–15.

11. **Li L, Zhao H, Chen B, Fan Z, Li N, Yue J, *et al.*** FXR activation alleviates tacrolimus-induced post-transplant diabetes mellitus by regulating renal gluconeogenesis and glucose uptake. J Transl Med 2019;17:1–10.

12. **Lim SW, Jin L, Piao SG, Chung BH, Yang CW.** Inhibition of dipeptidyl peptidase IV protects tacrolimus-induced kidney injury. Lab Investig 2015;95:1174–85.

13. **Gökçay Canpolat A, Şahin M.** Glucose Lowering Treatment Modalities of Type 2 Diabetes Mellitus. Adv Exp Med Biol 2021;1307:7–27. https://doi.org/10.1007/5584_2020_516.

14. **Mostafa DK, Khedr MM, Barakat MK, Abdellatif AA, Elsharkawy AM.** Autophagy blockade mechanistically links proton pump inhibitors to worsened diabetic nephropathy and aborts the renoprotection of metformin/enalapril. Life Sci 2021;265:118818. https://doi.org/10.1016/j.lfs.2020.118818.

15. **Bartlett F, January S, Pottebaum A, Horwedel T, Malone AF.** Impact of metformin on malignancy in solid organ transplantation. Clin Transplant 2020;34:e13851.

16. **Satriano J, Sharma K, Blantz RC, Deng A.** Induction of AMPK activity corrects early pathophysiological alterations in the subtotal nephrectomy model of chronic kidney disease. Am J Physiol Renal Physiol 2013;305:F727-33. https://doi.org/10.1152/ajprenal.00293.2013.

17. **De Broe ME, Jouret F.** Does metformin do more benefit or harm in chronic kidney disease patients? Kidney Int 2020;98:1098–101. https://doi.org/10.1016/j.kint.2020.04.059.

18. **Kajbaf F, Arnouts P, de Broe M, Lalau J.** Metformin therapy and kidney disease: a review of guidelines and proposals for metformin withdrawal around the world. Pharmacoepidemiol Drug Saf 2013;22:1027–35.

19. **ARAFA MAA, AMANY M.** Effect of Metformin Hydrochloride Administration and itsWithdrawal on the Kidneys of Adult Male Albino Rats: Histological and Biochemical Studies. Med J Cairo Univ 2021;89:337–54.

20. **Lalau J-D, Kajbaf F, Bennis Y, Hurtel-Lemaire A-S, Belpaire F, De Broe ME.** Metformin treatment in patients with type 2 diabetes and chronic kidney disease stages 3A, 3B, or 4. Diabetes Care 2018;41:547–53.

21. **Hadden MJ, Advani A.** Histone Deacetylase Inhibitors and Diabetic Kidney Disease. Int J Mol Sci 2018;19. https://doi.org/10.3390/ijms19092630.

22. **Rangwala S, Duvic M, Zhang C.** Trends in the treatment of cutaneous T-cell lymphoma–critical evaluation and perspectives on vorinostat. Blood Lymphat Cancer Targets Ther 2012;2:17–27.

23. **Batchu SN, Brijmohan AS, Advani A.** The therapeutic hope for HDAC6 inhibitors in malignancy and chronic disease. Clin Sci 2016;130:987–1003.

24. **Cabrera SM, Colvin SC, Tersey SA, Maier B, Nadler JL, Mirmira RG.** Effects of combination therapy with dipeptidyl peptidase-IV and histone deacetylase inhibitors in the non-obese diabetic mouse model of type 1 diabetes. Clin Exp Immunol 2013;172:375–82. https://doi.org/10.1111/cei.12068.

25. **Sharma S, Taliyan R.** Histone deacetylase inhibitors: Future therapeutics for insulin resistance and type 2 diabetes. Pharmacol Res 2016;113:320–6.

26. **Sevc J, Goldberg D, van Gorp S, Leerink M, Juhas S, Juhasova J, *et al.*** Effective long-term immunosuppression in rats by subcutaneously implanted sustained-release tacrolimus pellet: Effect on spinally grafted human neural precursor survival. Exp Neurol 2013;248:85–99. https://doi.org/10.1016/j.expneurol.2013.05.017.

27. **Hwang H, Ghee JY, Song JH, Piao S, Yang CW.** Comparison of adverse drug reaction profiles of two tacrolimus formulations in rats. Immunopharmacol Immunotoxicol 2012;34:434–42.

28. **Advani A, Huang Q, Thai K, Advani SL, White KE, Kelly DJ, *et al.*** Long-term administration of the histone deacetylase inhibitor vorinostat attenuates renal injury in experimental diabetes through an endothelial nitric oxide synthase-dependent mechanism. Am J Pathol 2011;178:2205–14. https://doi.org/10.1016/j.ajpath.2011.01.044.

29. **Gilbert RE, Huang Q, Thai K, Advani SL, Lee K, Yuen DA, *et al.*** Histone deacetylase inhibition attenuates diabetes-associated kidney growth: Potential role for epigenetic modification of the epidermal growth factor receptor. Kidney Int 2011;79:1312–21. https://doi.org/10.1038/ki.2011.39.

30. **Kerr JS, Galloway S, Lagrutta A, Armstrong M, Miller T, Richon VM, *et al.*** Nonclinical safety assessment of the histone deacetylase inhibitor vorinostat. Int J Toxicol 2010;29:3–19. https://doi.org/10.1177/1091581809352111.

31. **Cheng J-T, Huang C-C, Liu I-M, Tzeng T-F, Chang CJ.** Novel mechanism for plasma glucose–lowering action of metformin in streptozotocin-induced diabetic rats. Diabetes 2006;55:819–25.

32. **Quaile MP, Melich DH, Jordan HL, Nold JB, Chism JP, Polli JW, *et al.*** Toxicity and toxicokinetics of metformin in rats. Toxicol Appl Pharmacol 2010;243:340–7.

33. **Triggle CR, Mohammed I, Bshesh K, Marei I, Ye K, Ding H, *et al.*** Metformin: Is it a drug for all reasons and diseases? Metabolism 2022;133:155223. https://doi.org/https://doi.org/10.1016/j.metabol.2022.155223.

34. **Jin J, Lim SW, Jin L, Yu JH, Kim HS, Chung BH, *et al.*** Effects of metformin on hyperglycemia in an experimental model of tacrolimus- and sirolimus-induced diabetic rats. Korean J Intern Med 2017;32:314–22. https://doi.org/10.3904/kjim.2015.394.

35. **Hedenqvist P.** Laboratory animal analgesia, anesthesia, and euthanasia. Handb. Lab. Anim. Sci. 4th Editio, CRC press; 2021, p. 343–78.

36. **Zafar M, Naqvi SN-H.** Effects of STZ-Induced Diabetes on the Relative Weights of Kidney, Liver and Pancreas in Albino Rats: A Comparative Study. Int J Morphol 2010;28.

37. **Le J, Zhang X, Jia W, Zhang Y, Luo J, Sun Y, *et al.*** Regulation of microbiota-GLP1 axis by sennoside A in diet-induced obese mice. Acta Pharm Sin B 2019;9:758–68. https://doi.org/10.1016/j.apsb.2019.01.014.

38. **Mooli RGR, Mukhi D, Pasupulati AK, Evers SS, Sipula IJ, Jurczak M, *et al.*** Intestinal HIF-2α Regulates GLP-1 Secretion via Lipid Sensing in L-Cells. Cell Mol Gastroenterol Hepatol 2022;13:1057–72. https://doi.org/10.1016/j.jcmgh.2021.12.004.

39. **Bancroft JD, Layton C.** Connective and mesenchymal tissues with their stains. 8th Editio. Elsevier Amsterdam, The Netherlands; 2018.

40. **Shields VDC, Heinbockel T.** Introductory chapter: Histological microtechniques. Histology 2019:14.

41. **Kuloğlu HY.** Determination of reticular fibers in tissues fixed with sugarcane molasses. J Adv VetBio Sci Tech 2022;7:361–5.

42. **Ramos-Vara JA, Kiupel M, Baszler T, Bliven L, Brodersen B, Chelack B, *et al.*** Suggested guidelines for immunohistochemical techniques in veterinary diagnostic laboratories. J Vet Diagnostic Investig 2008;20:393–413.

43. **Özden H, Gömeç M, Şahin Y, Karaca G, Bulut H, Kilitçi A.** Protective effect of resveratrol on the kidney in rats under immunosuppression with tacrolimus. J Surg Med 2021;5:144–8.

44. **Fu R, Tajima S, Shigematsu T, Zhang M, Tsuchimoto A, Egashira N, *et al.*** Establishment of an experimental rat model of tacrolimus-induced kidney injury accompanied by interstitial fibrosis. Toxicol Lett 2021;341:43–50.

45. **Porrini E, Prieto MJ V, Fuentes MLD, Arevalo M, Ruiz ES, Torres A.** The Higher Diabetogenic Risk of Tacrolimus Depends on Pre-Existing Insulin Resistance. A Study Obese Lean Zucker Rats 2013;12:1665–75.

46. **Adikwu E, Nelson EC.** Assessments of kidney function and morphology of tramadol-diclofenac treated albino rats. Adv Life Sci 2018;5:104–12.

47. **Al-Rashidy AH, Salem RR, Alhosary AA, Wahdan MH, Elnemr GM, Hassan KE, *et al.*** Role of erythropoietin in methotrexate-induced nephrotoxicity in adult male albino rats. J Nephropharmacology 2018;7:156–63.

48. **Association AD. 2.** Classification and diagnosis of diabetes: standards of medical care in diabetes—2018. Diabetes Care 2018;41:S13–27.

49. **Quintana-Pérez JC, García-Dolores F, Valdez-Guerrero AS, Alemán-González-Duhart D, Arellano-Mendoza MG, Rojas Hernández S, *et al.*** Modeling type 2 diabetes in rats by administering tacrolimus. Islets 2022;14:114–27. https://doi.org/10.1080/19382014.2022.2051991.

50. **Albaghdadi AJH, Hewitt MA, Putos SM, Wells M, Ozolinš TRS, Kan FWK.** Tacrolimus in the prevention of adverse pregnancy outcomes and diabetes-associated embryopathies in obese and diabetic mice. J Transl Med 2017;15:1–15.

51. **Bakhdar FA.** Overview of New Onset Diabetes after Transplantation Induced by Tacrolimus. J Pharm Res Int 2021;32:14–26.

52. **Øzbay LA, Møller N, Juhl C, Bjerre M, Carstens J, Rungby J, *et al.*** Calcineurin inhibitors acutely improve insulin sensitivity without affecting insulin secretion in healthy human volunteers. Br J Clin Pharmacol 2012;73:536–45.

53. **Pérez-Flores I, Sánchez-Fructuoso A, Calvo N, Valga EF, Barrientos A.** Incidence and risk factors for the metabolic syndrome and posttransplant diabetes in renal transplant recipients taking tacrolimus. Transplant. Proc., vol. 42, Elsevier; 2010, p. 2902–4.

54. **Jenssen T, Hartmann A.** Emerging treatments for post-transplantation diabetes mellitus. Nat Rev Nephrol 2015;11:465–77. https://doi.org/10.1038/nrneph.2015.59.

55. **Seppi T, Prajczer S, Dörler M-M, Eiter O, Hekl D, Nevinny-Stickel M, *et al.*** Sex Differences in Renal Proximal Tubular Cell Homeostasis. J Am Soc Nephrol 2016;27:3051–62. https://doi.org/10.1681/ASN.2015080886.

56. **Zhang L, He Y, Wu C, Wu M, Chen X, Luo J, *et al.*** Altered expression of glucose metabolism associated genes in a tacrolimus-induced post-transplantation diabetes mellitus in rat model. Int J Mol Med 2019;44:1495–504. https://doi.org/10.3892/ijmm.2019.4313.

57. **Zhang Z, Sun J, Guo M, Yuan X.** Progress of new-onset diabetes after liver and kidney transplantation. Front Endocrinol (Lausanne) 2023;14:1091843.

58. **Jin J, Jin L, Luo K, Lim SW, Chung BH, Yang CW.** Effect of Empagliflozin on Tacrolimus-Induced Pancreas Islet Dysfunction and Renal Injury. Am J Transplant 2017;17:2601–16. https://doi.org/10.1111/ajt.14316.

59. **Li P, Zhang R, Zhou J, Guo P, Liu Y, Shi S.** Vancomycin relieves tacrolimus-induced hyperglycemia by eliminating gut bacterial beta-glucuronidase enzyme activity. Gut Microbes 2024;16:2310277. https://doi.org/10.1080/19490976.2024.2310277.

60. **Ewenighi C, Dimkpa U, Onyeanusi J, Onoh L, Onoh G, Ezugwu U.** Estimation of glucose level and body weight in Alloxan Induced Diabetic Rat treated with Aqueous extract of Garcinia Kola Seed. Ulutas Med J 2015;1:26–30.

61. **Danda RS, Habiba NM, Rincon-Choles H, Bhandari BK, Barnes JL, Abboud HE, *et al.*** Kidney involvement in a nongenetic rat model of type 2 diabetes. Kidney Int 2005;68:2562–71.

62. **Teoh SL, Latiff AA, Das S.** Histological changes in the kidneys of experimental diabetic rats fed with Momordica charantia (bitter gourd) extract. Rom J Morphol Embryol 2010;51:91–5.

63. **Cai H, Li G, Zhang P, Xu D, Chen L.** Effect of exercise on the quality of life in type 2 diabetes mellitus: a systematic review. Qual Life Res an Int J Qual Life Asp Treat Care Rehabil 2017;26:515–30. https://doi.org/10.1007/s11136-016-1481-5.

64. **Persaud SJ, Jones PM.** A Wake-up Call for Type 2 Diabetes? N Engl J Med 2016;375:1090–2. https://doi.org/10.1056/NEJMcibr1607950.

65. **Classification and Diagnosis of Diabetes:** Standards of Medical Care in Diabetes-2019. Diabetes Care 2019;42:S13–28. https://doi.org/10.2337/dc19-S002.

66. **Jouvet N, Estall JL.** The pancreas: Bandmaster of glucose homeostasis. Exp Cell Res 2017;360:19–23.

67. **Luo X, Wu J, Jing S, Yan L-J.** Hyperglycemic stress and carbon stress in diabetic glucotoxicity. Aging Dis 2016;7:90.

68. **Gonzalez-Franquesa A, Patti M-E.** Insulin resistance and mitochondrial dysfunction. Mitochondrial Dyn Cardiovasc Med 2017:465–520.

69. **Al-Awar A, Kupai K, Veszelka M, Szűcs G, Attieh Z, Murlasits Z, *et al.*** Experimental diabetes mellitus in different animal models. J Diabetes Res 2016;2016:9051426.

70. **Asrafuzzaman M, Cao Y, Afroz R, Kamato D, Gray S, Little PJ.** Animal models for assessing the impact of natural products on the aetiology and metabolic pathophysiology of Type 2 diabetes. Biomed Pharmacother 2017;89:1242–51.

71. **Krautz C, Wolk S, Steffen A, Knoch K-P, Ceglarek U, Thiery J, *et al.*** Effects of immunosuppression on alpha and beta cell renewal in transplanted mouse islets. Diabetologia 2013;56:1596–604.

72. **Shivaswamy V, Bennett RG, Clure CC, Ottemann B, Davis JS, Larsen JL, *et al.*** Tacrolimus and sirolimus have distinct effects on insulin signaling in male and female rats. Transl Res 2014;163:221–31. https://doi.org/https://doi.org/10.1016/j.trsl.2013.12.002.

73. **Heit JJ, Apelqvist ÅA, Gu X, Winslow MM, Neilson JR, Crabtree GR, *et al.*** Calcineurin/NFAT signalling regulates pancreatic β-cell growth and function. Nature 2006;443:345–9.

74. **Xu C, Niu Y-J, Liu X-J, Teng Y-Q, Li C-F, Wang H-Y, *et al.*** Tacrolimus reversibly reduces insulin secretion, induces insulin resistance, and causes islet cell damage in rats. Int J Clin Pharmacol Ther 2014;52:620–7.

75. **Øzbay LA, Smidt K, Mortensen DM, Carstens J, Jørgensen KA, Rungby J.** Cyclosporin and tacrolimus impair insulin secretion and transcriptional regulation in INS-1E beta-cells. Br J Pharmacol 2011;162:136–46.

76. **Tosur M, Viau-Colindres J, Astudillo M, Redondo MJ, Lyons SK.** Medication-induced hyperglycemia: pediatric perspective. BMJ Open Diabetes Res Care 2020;8:e000801.

77. **Uchizono Y, Iwase M, Nakamura U, Sasaki N, Goto D, Iida M.** Tacrolimus impairment of insulin secretion in isolated rat islets occurs at multiple distal sites in stimulus-secretion coupling. Endocrinology 2004;145:2264–72.

78. **Shivaswamy V, Bennett RG, Clure CC, Larsen JL, Hamel FG.** Metformin improves immunosuppressant induced hyperglycemia and exocrine apoptosis in rats. Transplantation 2013;95:280–4.

79. **Xie D, Guo J, Dang R, Li Y, Si Q, Han W, *et al.*** The effect of tacrolimus-induced toxicity on metabolic profiling in target tissues of mice. BMC Pharmacol Toxicol 2022;23:87.

80. **Inzucchi SE, Lipska KJ, Mayo H, Bailey CJ, McGuire DK.** Metformin in patients with type 2 diabetes and kidney disease: a systematic review. Jama 2014;312:2668–75.

81. **Hsu W-H, Hsiao P-J, Lin P-C, Chen S-C, Lee M-Y, Shin S-J.** Effect of metformin on kidney function in patients with type 2 diabetes mellitus and moderate chronic kidney disease. Oncotarget 2018;9:5416–23. https://doi.org/10.18632/oncotarget.23387.

82. **Khazaei M, Karimi J, Sheikh N, Goodarzi MT, Saidijam M, Khodadadi I, *et al.*** Effects of resveratrol on receptor for advanced glycation end products (RAGE) expression and oxidative stress in the liver of rats with type 2 diabetes. Phyther Res 2016;30:66–71.

83. **Tang Y, Choi E-J, Han WC, Oh M, Kim J, Hwang J-Y, *et al.*** Moringa oleifera from Cambodia ameliorates oxidative stress, hyperglycemia, and kidney dysfunction in type 2 diabetic mice. J Med Food 2017;20:502–10.

84. **Ribeiro T de P, Fonseca FL, de Carvalho MDC, Godinho RM da C, de Almeida FP, Saint'Pierre TD, *et al.*** Metal-based superoxide dismutase and catalase mimics reduce oxidative stress biomarkers and extend life span of Saccharomyces cerevisiae. Biochem J 2017;474:301–15.

85. **Moridi H, Karimi J, Sheikh N, Goodarzi MT, Saidijam M, Yadegarazari R, *et al.*** Resveratrol-dependent down-regulation of receptor for advanced glycation end-products and oxidative stress in kidney of rats with diabetes. Int J Endocrinol Metab 2015;13.

86. **Nasiri A, Ziamajidi N, Abbasalipourkabir R, Goodarzi MT, Saidijam M, Behrouj H, *et al.*** Beneficial effect of aqueous garlic extract on inflammation and oxidative stress status in the kidneys of type 1 diabetic rats. Indian J Clin Biochem 2017;32:329–36.

87. **Gao P, Du X, Liu L, Xu H, Liu M, Guan X, *et al.*** Astragaloside IV alleviates tacrolimus-induced chronic nephrotoxicity via p62-Keap1-Nrf2 pathway. Front Pharmacol 2021;11:610102.

88. **Oh SW, Kim S, Na KY, Chae D-W, Kim S, Jin DC, *et al.*** Clinical implications of pathologic diagnosis and classification for diabetic nephropathy. Diabetes Res Clin Pract 2012;97:418–24.

89. **Qi SS, Zheng HX, Jiang H, Yuan LP, Dong LC.** Protective Effects of Chromium Picolinate Against Diabetic-Induced Renal Dysfunction and Renal Fibrosis in Streptozotocin-Induced Diabetic Rats. Biomolecules 2020;10. https://doi.org/10.3390/biom10030398.

90. **El-Mahdy N, Elmasry T, El-Desouky K, Ghanem S.** The Renal and Cardio Protective Effects of Aliskiren and Pentoxifylline Alone and in Combination on Streptozotocin Induced Diabetic Rats. Br J Pharm Res 2016;12:1–11. https://doi.org/10.9734/BJPR/2016/26248.

91. **Al-Harbi NO, Imam F, Al-Harbi MM, Iqbal M, Nadeem A, Sayed-Ahmed MM, *et al.*** Olmesartan attenuates tacrolimus-induced biochemical and ultrastructural changes in rat kidney tissue. Biomed Res Int 2014;2014:607246.

92. **Donder E, Dogan MM, Kuloglu T, Dabak ÖD, Kocaman N, Ozkan Y.** The investigation of the effects of enalapril and losartan on ghrelin immunoreactivity in kidney of streptozotocin-induced diabetic rats. Fırat Tıp Derg 2013;18:1–6.

93. **Schlo D, Banas B.** The mesangial cell revisited: no cell is an island. J Am Soc Nephrol 2009;20:1179–87.

94. **Pourghasem M, Shafi H, Babazadeh Z.** Histological changes of kidney in diabetic nephropathy. Casp J Intern Med 2015;6:120.

95. **Sönmez MF, Dündar M.** Ameliorative effects of pentoxifylline on NOS induced by diabetes in rat kidney. Ren Fail 2016;38:605–13.

96. **Nagasaka S, Shimizu A.** Experimental Animal Models of Diabetic Kidney Disease. Diabet Kidney Dis 2021:173–90.

97. **Zhou C, Vink R, Byard RW.** Hyperosmolarity induces Armanni-Ebstein-like renal tubular epithelial swelling and cytoplasmic vacuolization. J Forensic Sci 2017;62:229–32.

98. **Adaramoye O, Akanni O, Adesanoye O, Ambali O, Olaremi O.** Evaluation of toxic effects of metformin hydrochloride and glibenclamide on some organs of male Rats. Niger J Physiol Sci 2012;27:137–44.

99. **Citro A, Valle A, Cantarelli E, Mercalli A, Pellegrini S, Liberati D, *et al.*** CXCR1/2 inhibition blocks and reverses type 1 diabetes in mice. Diabetes 2015;64:1329–40.

100. **Fareed SA, Yousef EM, Abd El-Moneam SM.** Assessment of Effects of Rosemary Essential Oil on the Kidney Pathology of Diabetic Adult Male Albino Rats. Cureus 2023;15:e35736. https://doi.org/10.7759/cureus.35736.

101. **Geraldes P, King GL.** Activation of protein kinase C isoforms and its impact on diabetic complications. Circ Res 2010;106:1319–31.

102. **Kidokoro K, Satoh M, Nagasu H, Sakuta T, Kuwabara A, Yorimitsu D, *et al.*** Tacrolimus Induces Glomerular Injury via Endothelial Dysfunction Caused by Reactive Oxygen Species and Inflammatory Change. Kidney Blood Press Res 2012;35:549–57. https://doi.org/10.1159/000339494.

103. **Panizo S, Martínez-Arias L, Alonso-Montes C, Cannata P, Martín-Carro B, Fernández-Martín JL, *et al.*** Fibrosis in Chronic Kidney Disease: Pathogenesis and Consequences. Int J Mol Sci 2021;22. https://doi.org/10.3390/ijms22010408.

104. **Reiss AB, Jacob B, Zubair A, Srivastava A, Johnson M, De Leon J.** Fibrosis in Chronic Kidney Disease: Pathophysiology and Therapeutic Targets. J Clin Med 2024;13. https://doi.org/10.3390/jcm13071881.

105. **Bülow RD, Boor P.** Extracellular Matrix in Kidney Fibrosis: More Than Just a Scaffold. J Histochem Cytochem Off J Histochem Soc 2019;67:643–61. https://doi.org/10.1369/0022155419849388.

106. **Mohammad HMF, Galal Gouda S, Eladl MA, Elkazaz AY, Elbayoumi KS, Farag NE, *et al.*** Metformin suppresses LRG1 and TGFβ1/ALK1-induced angiogenesis and protects against ultrastructural changes in rat diabetic nephropathy. Biomed Pharmacother 2023;158:114128. https://doi.org/https://doi.org/10.1016/j.biopha.2022.114128.

107. Choi HS, Song JH, Kim IJ, Joo SY, Eom GH, Kim I, *et al.* Histone deacetylase inhibitor, CG200745 attenuates renal fibrosis in obstructive kidney disease. Sci Rep 2018;8:11546.

108. Khan S, Jena G. Sodium butyrate, a HDAC inhibitor ameliorates eNOS, iNOS and TGF-β1-induced fibrogenesis, apoptosis and DNA damage in the kidney of juvenile diabetic rats. Food Chem Toxicol 2014;73:127–39.

109. Liu N, He S, Ma L, Ponnusamy M, Tang J, Tolbert E, *et al.* Blocking the class I histone deacetylase ameliorates renal fibrosis and inhibits renal fibroblast activation via modulating TGF-beta and EGFR signaling. PLoS One 2013;8:e54001.

110. Wang F, Sun H, Zuo B, Shi K, Zhang X, Zhang C, *et al.* Metformin attenuates renal tubulointerstitial fibrosis via upgrading autophagy in the early stage of diabetic nephropathy. Sci Rep 2021;11:16362.

111. Luo K, Lim SW, Jin J, Jin L, Gil HW, Im DS, *et al.* Cilastatin protects against tacrolimus-induced nephrotoxicity via anti-oxidative and anti-apoptotic properties. BMC Nephrol 2019;20:1–11.

112. Kim HS, Lim SW, Jin L, Jin J, Chung BH, Yang CW. The protective effect of febuxostat on chronic tacrolimus-induced nephrotoxicity in rats. Nephron 2017;135:61–71.

113. Pu J, Liu T, Wang X, Sharma A, Schmidt-Wolf IGH, Jiang L, *et al.* Exploring the role of histone deacetylase and histone deacetylase inhibitors in the context of multiple myeloma: mechanisms, therapeutic implications, and future perspectives. Exp Hematol Oncol 2024;13:45.

التأثير الوقائي المحتمل للفورينوستات مقابل الميتفورمين على نموذج الجرذان لمرض السكري الجديد المستحدث بعد الزرع: دراسة نسيجية ومناعية نسيجية كيميائية وكيميائية حيوية

هبة فكري[١]، لبنى أحمد صالح[٢]، هدوي علي عبد الخالق[١] و دعاء رمضان صادق[١]

[١]قسم الهستولوجى [٢]قسم الأدويه الاكلينيكية، كلية الطب، جامعة عين شمس، القاهر، مصر

المقدمة: التاكروليموس هو أحد أكثر الأدوية المثبطة للمناعة شيوعًا و المستخدمة في زراعة الأعضاء. بعد زراعة الأعضاء قد يصاب المريض بمرض السكري الجديد المستحدث بعد الزرع. كما يعد تأثير دواء الميتفورمين على مرض السكري الذي يظهر حديثًا بعد زراعة الأعضاء بسبب العلاج بمثبطات المناعة غير مفهوم جيدًا، و ذلك على الرغم من أنه يعد دواء الخط الأول لعلاج مرض السكري من النوع الثاني.

الهدف من البحث: لذلك، تهدف الدراسة الحالية إلى دراسة التأثيرات الوقائية المحتملة للفورينوستات مقارنة بالميتفورمين في اعتلال الكلية السكري في نموذج السكري الجديد بعد الزرع في الجرذان باستخدام التاكروليموس.

المواد وطرق البحث: تم تقسيم اثنين وأربعين من ذكور الجرذان ويستار البيضاء البالغة بشكل عشوائي إلى ست مجموعات: المجموعة الضابطة، مجموعة الفورينوستات، مجموعة الميتفورمين، مجموعة نموذج مرض السكري الجديد بعد الزرع و والمجموعة المعالجة ب الفورينوستات و المجموعة المعالجة بالميتفورمين. تم إعطاء جرعة عالية من التاكروليموس يوميا عن طريق الحقن تحت الجلد لمدة أربعة أسابيع. كما تم إعطاء الفورينوستات والميتفورمين عن طريق الفم يوميا بالتزامن مع إعطاء التاكروليموس في المجموعتين الخامسة والسادسة. في نهاية التجربة بعد أربعة أسابيع، تم تجميع عينات الدم لقياس وظائف الكلى. كما تم تجميع عينات الكلى ووزنها ثم عمل الدراسات النسيجية والهستوكيميائية المناعية والقياسية بالإضافة الى قياس علامات الإجهاد التأكسدي.

النتائج: أظهرت مجموعة نموذج الجرذان لمرض السكري الجديد المستحدث بعد الزرع زيادة واضحة في الوزن النسبي لكلى، وقد أدى إعطاء الفورينوستات إلى تقليل الوزن النسبي لكلى الجرذان. كشفت نتائج كل من الهيماتوكسلين والايوسين، صبغة ماسون ثلاثية الألوان، و صبغة جوردن وسويت، و تفاعل حمض الفوق ايودي و كاشف شيف لتشريب الفضة عن إصابات في الكلى تم تأكيدها إحصائيًا. كما أظهرت الدراسة الحالية أن الجرذان التي تم أعطاؤها تاكروليموس كعالج الوحيد لكليتيهم كانت لديها مستويات أعلى بشكل ملحوظ من الكاسبيز٣- لخاليا الأنابيب القريبة. وقد تم تخفيض هذه النسبة بشكل كبير في الجرذان التي عولجت باستخدام الفورينوستات. النتيجة الأكثر أهمية لهذه الدراسة هي أن عالج الفورينوستات أو الميتفورمين تسبب ا في تأثيرات مختلفة لخفض مستوى الجلوكوز في الدم. قام الميتفورمين بتحسين هذه النسبة، ولكن ليس بالدرجة التي شوهدت مع الفورينوستات.

الاستنتاج: أظهرت نتائج الدراسة الحالية أن الفورينوستات كان أفضل من الميتفورمين في الوقاية من تلف الكلى في نموذج السكري المستحدث بعد زراعة الأعضاء الناتج من إعطاء التاكروليموس. ظهر هذا من خلال زيادة القدرة المضادة للأكسدة وتقليل الضرر التأكسدي، و تقليل موت الخلايا المبرمج. لذلك، أظهر الفورينوستات تأثيرا مزدوجا: فقد منع تلف الكلى وحسن النتائج البيوكيميائية.